Aus der Medizinischen Klinik und Poliklinik II

der Universität Würzburg

Direktor: Professor Dr. med. Einsele

Analyse von MicroRNA-Profilen in humanen dendritischen Zellen

Inaugural - Dissertation

zur Erlangung der Doktorwürde der

Medizinischen Fakultät

der

Julius-Maximilians-Universität Würzburg

vorgelegt von

Mithun Das Gupta

aus Hiltenfingen

Würzburg, August 2013

Referent:	Priv.-Doz. Dr. Jürgen Löffler
Koreferent:	Prof. Dr. Matthias Eyrich
Dekan:	Prof. Dr. Frosch

Tag der mündlichen Prüfung: 27.11.2014

Der Promovend ist Arzt.

Table of contents

1. Introduction

1.1. MiRNA

1.1.1. Discovery

The discovery of microRNA (miRNA) opened up a new chapter in the field of gene expression regulation. This class of single stranded, approximately 22 nucleotides (nt) long RNAs act as posttranscriptional gene regulators and a member of this class was first described in 1993 (Lee et al.). The authors revealed that lin-4, a gene that is essential for the control of postembryonic development in Caenorhabditis elegans by down-regulation of LIN-14 protein (Arasu et al. 1991), does not encode a protein, but two small RNAs. The larger transcript, named lin-4L, was found to be approximately 61 nt in length and the smaller transcript, lin-4S, was estimated to be 22 nt long. The facts that lin-4S was identical in sequence to the first 22 nucleotides of lin-4L and that the secondary sequence of lin-4L was predicted to be unfavorable for its function, lead to the assumption that the larger transcript might be a precursor of the smaller one (Lee et al. 1993; Bartel 2004). Interestingly, the lin-4 transcripts showed antisense complementarity to seven sites of the 3'-untranslated region (3'-UTR) of lin-14 (Lee et al. 1993; Wightman et al. 1993). Wightman et al. also confirmed that the 3'-UTR of lin-14 was both necessary and sufficient to mediate lin-4 dependant posttranscriptional regulation of the LIN-14 protein. The down-regulation of lin-14 by lin-4 resulted in a substantial reduction in the amount of LIN-14 protein, but had only minor effects on the expression of lin-14 mRNA, supporting a hypothesis of posttranscriptional gene regulation (Wightman et al. 1991; Wightman et al. 1993).

On the basis of these findings, a model of posttranscriptional repression by direct RNA to RNA interaction of lin-4S or lin-4L and lin-14 mRNA was proposed (Lee et al. 1993; Wightman et al. 1993). Thus these authors correctly described the function of lin-4S, a 22 nt long small RNA, which is now widely regarded as the first discovered miRNA (Bartel 2004). Since then, about 400 miRNA genes have been identified in humans (Bartel 2009). MiRNAs have been found to play pivotal roles in many different fields

including cancer biology (Cortez et al. 2010; Farazi et al. 2011), immunology and infectious diseases (Dai and Ahmed 2011; O'Neill et al. 2011). However, up until now, this is the first study that investigates miRNA-profiles of dendritic cells in response to fungal infection by *Aspergillus fumigatus* (*A. fum*).

1.1.2. Biogenesis and function

The first miRNA precursor molecules, called pri-miRNAs, are transcribed from DNA segments that are either introns of protein coding genes or exons or introns of noncoding genes, or lie within intergenic regions and code for a single or multiple RNAs by polymerase II (Cai et al. 2004; Lee et al. 2004; van Rooij 2011). In humans, pri-miRNAs are processed in the nucleus by drosha, a member of the RNase III superfamily, into 60-100 nt long hairpin stem-loop precursors named pre-miRNAs (Lee et al. 2003; van Rooij 2011). Drosha acts as part of a larger complex, often described as the microprocessor complex (Denli et al. 2004; Gregory et al. 2004). The pre-miRNA is exported to the cytoplasm via exportin 5 (Yi et al. 2003; Yi et al. 2005). There it is cleaved by the enzyme dicer, like drosha a RNase III endonuclease, which results in an imperfect duplex structure consisting of the future, mature miRNA strand and a miRNA* fragment derived from the complementary stem-loop arm of the pre-miRNA (Bartel 2004). The duplex is separated by a yet undefined helicase and the mature miRNA is incorporated into a RNA-induced silencing complex (RISC), whereas the miRNA* strand is usually degraded (Bartel 2004; van Rooij 2011). Directed by the miRNA, the RISC may impair gene expression by two pathways. It may either lead to the cleavage of the target mRNA or solely bind to it and thereby interfere with translation, a mechanism named translational repression. After disrupting a target mRNA, the RISC complex remains intact and is able to destroy further mRNAs. Among other factors and excluding some exceptions, the level of complementarity between the miRNA and the target mRNA seems to determine whether a mRNA is cleaved or translationally repressed (Bartel 2004; Huntzinger and Izaurralde 2011). Recent studies support the assumption that mRNA degradation is the main mechanism by which miRNAs regulate protein levels in mammalian cells (Huntzinger and Izaurralde 2011).

1.1.3. Medical use

Due to their involvement in many biological processes, it stands to reason that miRNAs have a huge potential for medical diagnostics and therapeutics. So far, several studies have evaluated the measurement of different miRNAs as biomarkers in disease (Cortez and Calin 2009; Cortez et al. 2011). A recent study analysed miRNA profiles of lung tumors, normal lung tissue and plasma samples from patients and healthy individuals enrolled in a screening trial (Boeri et al. 2011). It was found that the miRNA expression pattern of tumor tissue strongly differed from the expression in normal lung tissue. Certain expression profiles could be associated with different tumor histology and growth rate. Furthermore, expression profiles correlated with clinical outcome and year of lung cancer CT detection in individuals from the screening trial. These findings highlight the value of miRNA as a tool for risk evaluation and stratification, diagnosis and prognosis for many diseases.

MiRNA function may be directly targeted by therapeutic agents via two pathways, namely the introduction of so called anti-miRs, antisense oligonucleotides that specifically bind to their corresponding miRNA, or by miRNA mimicry using synthetic miRNAs (van Rooij 2011).

Anti-miRs require various properties to effectively reach and suppress their target miRNA in vivo. In addition to high specifity and affinity for their target, the anti-miRs should possess sufficient cell permeability and stability in vivo. Mainly two chemical modifications have been used so far to achieve these goals. One is the introduction of a 2'-O-methyl group into the oligonucleotide compound, the other one enhances stability by linking the 2'-O-oxygen to the 4' position with the help of a methylene molecule, producing so called LNA-modified oligonucleotides (van Rooij 2011). In a recently published clinical study, treatment with miravirsen, a LNA-modified anti-miR targeting miR-122, lead to substantial decreases in HCV RNA plasma levels in patients with chronic HCV genotype 1 infection (Janssen et al. 2013).

To this date, miRNA mimicry has been accomplished by the use of synthetic RNA duplexes and by the introduction of miRNA via viral vectors. The synthetic duplex

usually consists of a strand that is identical to a specific miRNA and another strand which is modified to meet chemical requirements for cell permeability and stability (van Rooij 2011). As for the use of viral vectors, a study from 2009 serves as an extraordinarily promising example. It was shown that in a mouse model of hepatocellular carcinoma, the expression of miR-26a in cancer cells cannot only be substituted with the help of an adeno-associated virus as a vector, but that this substitution also results in an effective inhibition of cancer cell proliferation (Kota et al. 2009).

In view of the emerging importance of miRNA in medical diagnosis and therapy, it seems justified to hope that a study of miRNA profiles in immune cells stimulated with *A. fum* might contribute to the establishment of miRNAs as diagnostic markers, risk stratification tools or therapeutic targets in aspergillosis or other infectious or immunologic diseases.

1.2. Invasive fungal infections

1.2.1. Epidemiology

Invasive aspergillosis (IA) is the most common cause of mortality due to infection in patients treated for hematological malignancies and is an emerging disease in solid organ transplant recipients and in patients receiving novel immunomodulatory therapies (Marr 2010). Data from 23 transplant centers in the United States, covering the epidemiology of invasive fungal infections (IFIs) in hematopoietic stem cell transplantation (HSCT) patients and solid organ transplant (SOT) recipients, granted the first broad multicenter insight into fungal infections in this population. The incidence of IFIs in HSCT patients was reported to be 3.4 %, with aspergillosis accounting for 43 % and candidiasis accounting for 28 % of these infections. Fusarium, Scedosporium and Zygomycetes were responsible for the remainder of infections. IA was associated with a one year survival rate of only 25 %. In all SOT recipients except lung transplant recipients, Candida infections were higher in incidence than Aspergillus infections. Patient having undergone lung transplantation had higher rates of IA than candidiasis (Person et al. 2010). There appears to be no recent data on the

epidemiology of IFIs in the general oncology population. An autopsy study from 1992 found fungal infections in 25 % of patients with leukemia, in 12 % of lymphoma patients and in 5 % of patients with solid tumors, with Candida being responsible for 58 % and Aspergillus being responsible for 30 % of infections (Bodey et al. 1992; Person et al. 2010).

1.2.2. Aspergillosis

Aspergillus fumigatus is a filamentous, saprophytic fungus (mold) that naturally lives in the soil and grows on organic waste. It produces scores of conidia which are released into the atmosphere. The ubiquitous airborne conidia have a diameter of 2 – 3 µm, a size that allows them to reach the lung alveoli when inhaled by humans. In immunocompetent persons, inhaled conidia are usually efficiently eliminated by innate immunity (Latgé 1999; Segal 2009).

In immunocompetent individuals, Aspergillus may be responsible for various allergic disorders, such as allergic sinusitis, asthma and farmer's lung. Colonization of bronchial airways may lead to recurrent inflammation with transient pulmonary infiltrates and airway plugging, a severe disorder named allergic bronchopulmonary aspergillosis (Latgé 1999; Segal 2009).

Invasive aspergillosis is a disease that affects persons with a compromised immune system. Clinical and histological features of the disease vary with predisposing host factors. In patients with neutropenia resulting from high-dose chemotherapy or underlying hematolgic disease, rapid hyphal angioinvasion with thrombosis and tissue infarction may occur. Due to the lack of effector cells, the inflammatory response is low. Individuals receiving immunosuppressive therapy for GVHD or after SOT are susceptible for infection with *A. fum* that commonly presents as pneumonia (Segal 2009).

The diagnosis of IA remains challenging as neither clinical or radiological signs show sufficient specifity, and sputum cultures lack sensitivity (Segal 2009). The revised definitions of the EORTC/MSG Consensus Group demand histopathologic evidence or positive cultures from defined specimen for the diagnosis of proven invasive fungal

disease (IFD). The criteria for probable IFD include host factors (e.g. history of neutropenia), clinical criteria and mycological criteria. For IA the mycological criteria consist of the detection of galactomannan antigen in defined specimen and β-D-glucan detection in serum. The category of possible IFD was outlined for patients with matching host factors and clinical evidence but without mycological indications (de Pauw et al., 2008). It is expected that new PCR-based methods and biomarker tools detecting signs of fungal infection in body specimen will enhance diagnostic accuracy in future (Chen and Kontoyiannis 2010).

For the treatment of invasive pulmonary aspergillosis, the Infectious Diseases Society of America (IDSA) recommends voriconazole as the medication of choice. As a salvage therapy for patients who are refractory to or intolerant of voriconazole, the Society's guidelines advice the use of lipid formulations of amphotericin B, caspofungin or other azoles (Walsh et al. 2008). Patients at high risk for IA benefit from empirical or preemptive therapy and from antifungal prophylaxis. The IDSA recommends empirical antifungal therapy for patients with persistent or recurrent fever after 4-7 days of antibiotic therapy and who are expected to suffer from neutropenia for longer than 7 days. Alternatively, a preemptive approach guided by clinical signs, CT signs and serologic results, is described as acceptable. Prophylaxis against IA is warranted for patients receiving intensive chemotherapy for the treatment of AML or MDS (Freifeld et al. 2011).

1.3. Host defense to *A. fum* and dendritic cells

Macrophages and polymorphonuclear leucocytes (PMNLs) constitute the first line of defense against conidia of *A. fum* that enter the respiratory tract. Alveolar macrophages phagocytose conidia and disrupt them with reactive oxygen intermediates (ROIs) generated by the enzyme NADPH-oxidase (Philippe et al. 2003). PMNLs inhibit conidial germination by releasing lactoferrin (Bonnett et al. 2006; Zarember et al. 2007). In addition, various soluble molecules, e.g. lysozyme and surfactant proteins, partake in the innate immune defense against *A. fum* (Ben-Ami et al. 2010). Should conidia still evolve to germ tubes and hyphae, the fungus becomes

too large to be phagocytosed by macrophages. Accumulating PMNLs remain effective, and attack the fungal hyphae with the release of ROIs and further mechanisms (Levitz and Farrell 1990; Rex et al. 1990; Levitz 2004; Ben-Ami et al. 2010).

On a cellular level, components of *A. fum*, especially the cell wall constituents β-glucan, chitin and galactomannan, are recognized by various pattern recognition receptors (PRRs) on the host cell. In general, these receptors recognize conserved structures on microorganisms (Gresnigt et al. 2012). The soluble receptor pentraxin-3 (PTX-3) for example stimulates the activity of macrophages and dendritic cells against conidia (Ben-Ami et al. 2010). Dectin-1, a receptor on PMNLs, alveolar macrophages and dendritic cells ligates the cell wall component β-glucan (Brown and Gordon 2001). The Toll-like receptors TLR2 and TLR4 are essential for the recognition of *A. fum* by macrophages, even though their fungal ligands have not been characterized yet (Wang et al. 2001; Mambula et al. 2002; Meier et al. 2003; Bellocchio et al. 2004). A receptor named DC-SIGN is specifically found on dendritic cells and binds to galactomannan (Serrano-Gómez et al. 2004). Dendritic cells (DCs) also function as the crucial initiators of adaptive immunity against *A. fum* (Ben-Ami et al. 2010). They encounter antigens like cell wall components of *A. fum* in the periphery, upon which they enter a process of maturation. During maturation, DCs coordinately take up antigens and process them for presentation. In addition, expression of costimulatory molecules and cytokines is up-regulated (Lanzavecchia and Sallusto 2001). The maturating DCs migrate to secondary lymphoid organs where they present antigen-specific, co-stimulatory and Th1/Th2 polarizing signals to T helper cells. Polarization of T helper cells by DCs is dependent on various factors, including DC subsets and the morphology of *A. fum* (Netea et al. 2006). The presence of DCs in germinal centers and further evidence suggests that DCs also play a role in B cell stimulation (Lanzavecchia and Sallusto 2001). A Th1 biased response to *A. fum* appears to be pivotal for effective immunity (Ben-Ami et al. 2010). Cenci et al. (1997) found that a marked Th1 response in mice had a beneficial effect on the resistance to IA, whereas Th2-type lymphocytes promoted the development of allergic bronchopulmonary aspergillosis. A study by Hebart et al. (2002), that investigated cytokine patterns in patients with IA, revealed

that an increase in Th1-type cytokines compared to Th-2 type cytokines was linked to a better outcome.

The present study introduces miRNAs as new players in the cellular response of DCs to different morphologies of *A. fum*.

2. Materials and Methods

2.1. Laboratory equipment

Instrument	Name/Model	Manufacturer
Centrifuges	Centrifuge 5415 R Heraeus® Multifuge® 3SR Galaxy Mini MC-6400 Centrifuge Rotanta 46 RC	Eppendorf Thermo Scientific VWR Hartenstein Hettich
ELISA reader	Model 680 Microplate Reader	Bio-Rad
Freezers	KGK 2833 Comfort Herafreeze HFU3280HD	Liebherr Thermo
Incubator	Heraeus BBD 6220	Thermo/Kendro
MACS® Separator	QuadroMACS™ Separator	Miltenyi Biotec
Manifold dispenser	Manifold Dispenser 300	Eppendorf
Microplate reader	680 Microplate Reader	Bio-Rad
Microscopes	Eclipse 50i Eclipse TS100	Nikon Nikon
Neubauer haemocytometer	Neubauer Improved	HBG Henneberg-Sander
Pipettes	Eppendorf Reference® (2.5 µl, 10 µl, 100 µl, 1000 µl) Multipette® plus	Eppendorf Eppendorf
Pipetting aid	Pipetus®	Hirschmann
Real-time PCR system	StepOnePlus™	Applied Biosystems
Shaker	HydroFlex™	Tecan
Shaker-incubator	Stuart SI500 Shaking Incubator	Stuart®

Instrument	Name/Model	Manufacturer
Spectrophotometer	NanoDrop 1000	Peqlab
Thermal cycler	Applied Biosystems 9800 Fast Thermal Cycler	Applied Biosystems
Vortexer	Vortex Genie 2	Scientific Industries
Workbench	Herasafe HS 15	Heraeus/Kendro

Table 1

2.2. Single use items

Item	Label	Manufacturer
Cell scrapers	Cell Scraper steril	A. Hartenstein
Cell strainers	BD Falcon™ Cell Strainer, 40 µm	BD Biosciences
MACS® Cell Separation Columns	LS Column	Miltenyi Biotec
Microplates for ELISA	Microplate, 96 well	Greiner Bio-One
Optical adhesive cover/sealing strip	Sealing tape, optically clear ELISA Plate Sealers	Sarstedt R&D Systems®
Pasteur's pipettes	Pasteur's pipette 3 ml steril	A. Hartenstein
Pipette tips	TipOne Tips (10 µl, 100 µl, 1000 µl)	StarLab
Serological pipettes	Serological Pipette (2 ml, 5 ml, 10 ml, 25 ml, 50ml)	Greiner Bio-One
Tissue Culture Flasks	75 ml CellStar® Tissue Culture Flask	Greiner Bio-One

Item	Label	Manufacturer
Tubes	BD Falcon™ Conical Tube (15 ml, 50 ml) FlipTube (0.2 ml, 1.5 ml, 2 ml)	BD Biosciences A. Hartenstein
Well plates	Multiwell™ 6 well Multiwell™ 24 well MicroAmp™ 96 well Tray for VeriFlex™ Blocks	BD Biosciences BD Biosciences Applied Biosystems

Table 2

2.3. Assays and kits

Assay/Kit	Components	Manufacturer
*mir*Vana™ miRNA Isolation Kit	Wash Solution 1 Wash Solution 2/3 Collection Tubes Filter Cartridges Lysis/Binding Buffer miRNA Homogenate Additive	Ambion®/Applied Biosystems
TaqMan® MiRNA Reverse Transcription Kit	100 mM dNTPs MultiScribe™ Reverse Transcriptase, 50 $\frac{U}{\mu l}$ 10X RT Buffer RNase Inhibitor	Applied Biosystems
TaqMan® MiRNA Assay (for miR-132, miR-146a, miR-155)	5X Reverse Transcription Primer 20X Real-Time PCR Assay	Applied Biosystems

Assay/Kit	Components	Manufacturer
Human CCL20/MIP-3α Quantikine® ELISA Kit	see 2.4	R&D Systems®
Human IL-1β/IL-1F2 Quantikine® ELISA Kit	see 2.4	R&D Systems®
Human IL-6 Quantikine® ELISA Kit	see 2.4	R&D Systems®

Table 3

2.4. Reagents, solutions and buffers

Reagent/Solution/Buffer	Details	Manufacturer
Blocking buffer (ELISA)	500 ml PBS 25 ml Sucrose 5 ml BSA (Albumin Fraction V) 0.25 ml sodium azide	Sigma-Aldrich Calbiochem®, Merck Roth Merck
EDTA	Ethylenediaminetetraacetic acid disodium salt solution, 0.5 M	Sigma-Aldrich
Ethanol	Absolute	Sigma-Aldrich
FCS	Fetal Calf Serum	Sigma-Aldrich
Ficoll®	Biocoll separating solution, density 1.077 $\frac{g}{ml}$	Biochrom
Hanks	500 ml HBSS 5 ml FCS 2 ml EDTA	Gibco®/Invitrogen Sigma-Aldrich Sigma-Aldrich
HBSS	Hank's Balanced Salt Solution	Gibco®/Invitrogen
PBS	Phosphate buffered saline	Sigma-Aldrich

Reagent/Solution/Buffer	Details	Manufacturer
PCR master mix	TaqMan® 2X Universal PCR Master Mix	Applied Biosystems
Phenol: chloroform: isoamylalcohol	Ratio 25: 24: 1	Ambion®/Applied Biosystems
Refobacin	Gentamicin sulfate	Merck
RPMI medium 1640	Contains GlutaMAX™-I (glutamine)	Gibco®/Invitrogen
Standard buffer 1 (ELISA)	500 ml PBS 0.5 ml BSA (Albumin Fraction V)	Sigma-Aldrich Roth
Standard buffer 2 (ELISA)	20 mM Trizma® base 150 mM sodium chloride 0.1 % BSA (Albumin Fraction V)	Sigma-Aldrich Riedel-de Haen, Honeywell Roth
Standard buffer 3 (ELISA)	500 ml PBS 5 ml BSA (Albumin Fraction V)	Sigma-Aldrich Roth
Streptavidin-HRP	Streptavidin conjugated to horseradish peroxidase	R&D Systems®
Substrate solution (ELISA)	5280 µl color reagent A 5280 µl color reagent B (both from substrate reagent pack)	R&D Systems®
Trypan blue	0.4 %	Sigma-Aldrich
Wash buffer (ELISA)	500 ml PBS 1ml Tween® 20	Sigma-Aldrich Sigma-Aldrich

Table 4

2.5. Cytokines, TLR-ligands and antibodies

Cytokine/TLR-Ligand/ Antibody	Details	Manufacturer
Biotinylated CCL20/MIP-3α antibody	Monoclonal, anti-human (detection antibody for ELISA)	R&D Systems®
Biotinylated IL-1β/IL-1F2 antibody	Monoclonal, anti-human (detection antibody for ELISA)	R&D Systems®
Biotinylated IL-6 antibody	Monoclonal, anti-human (detection antibody for ELISA)	R&D Systems®
CCL20/MIP-3α	Recombinant, human	R&D Systems®
CCL20/MIP-3α antibody	Monoclonal, anti-human (capture antibody for ELISA)	R&D Systems®
CD14 Microbeads	Microbeads conjugated to antihuman CD14 antibodies	Miltenyi Biotec
GM-CSF	Leukine® (sargramostim), recombinant human granulocyte-macrophage colony-stimulating factor	Bayer
IL-1β/IL-1F2	Recombinant, human	R&D Systems®
IL-1β/IL-1F2 antibody	Monoclonal, anti-human (capture antibody for ELISA)	R&D Systems®
IL-4	Recombinant human interleukin-4	R&D Systems®
IL-6	Recombinant, human	R&D Systems®

Cytokine/TLR-Ligand/ Antibody	Details	Manufacturer
IL-6 antibody	Monoclonal, anti-human (capture antibody for ELISA)	R&D Systems®
LPS	Ultrapure lipopolysaccharide, E. coli0111:B4	InvivoGen
Zymosan	Cell wall from Saccharomyces cerevisiae	InvivoGen
Zymosan depleted	Hot alkali treated cell wall from Saccharomyces cerevisiae	InvivoGen

Table 5

2.6. Culture media

Medium	Components
Beer mash plates	Beer mash (The prepared agar plates were kindly supplied by the Institute for Hygiene and Microbiology, University of Würzburg.)
RPMI medium for cells	90 % RPMI medium 1640 10 % FCS 0.12 $\frac{g}{l}$ Refobacin
RPMI medium for fungus	80 % RPMI medium 1640 20 % FCS

Table 6

2.7. Generation of monocyte derived dendritic cells

As the first step towards the generation of human monocyte-derived dendritic cells (moDCs), peripheral blood mononuclear cells (PBMCs) were isolated from leucocyte

concentrates by density gradient centrifugation. The leucocyte concentrates were produced from the blood of healthy donors and kindly supplied by the Institute for Transfusion Medicine and Haemotherapy, University of Würzburg. Initially a leucocyte concentrate (usually 10 ml) was diluted with Hanks at a ratio of 1:9. Then 25 ml of the deluted concentrate were carefully applied over 20 ml Ficoll® in a 50 ml Falcon™ tube. The processing of one leucocyte concentrate usually resulted in four 50 ml tubes. The tubes were then centrifuged for 10 min at a speed of 2000 rpm. After centrifugation the tubes showed three layers: plasma, interphase enriched with PBMCs and Ficoll® with erythrocytes and polymorphonuclear cells. The interphases were taken with a Pasteur's pipette and transferred into two 50 ml Falcon® tubes. As a first washing step the tubes were filled with Hanks up to the 50 ml mark and subsequently centrifuged for 10 min at 1214 rpm. Next, the supernatants in the tubes were decanted and the remaining cell pellets were resuspended in 50 ml Hanks and pooled into one tube. In order to determine the cell count, 20 µl were taken from the cell suspension and added to 180 µl of Hanks (1:10 dilution). This suspension was then further diluted with trypan blue, a vital stain, at a ratio of 1:1. After that, a prepared Neubauer haemocytometer was filled with the stained cell suspension and the cells were counted under the microscope. The cell count was then calculated by the formula

$$x \times \frac{10^4}{ml} \times 50\ ml \times 10 \times 2,$$

where x is the number of cells counted in a defined square area of the Neubauer haemocytometer grid and the factors 10 and 2 account for the two dilution steps. Hereafter the second wash step was completed by centrifugation (10 min at 1214 rpm) and subsequent decantation of the 50 ml cell suspension. The remaining cell pellet with the known number of PBMCs (usually ranging between 5×10^8 and 15×10^8) was then suspended in Hanks so that the cell concentration is 2.9×10^8 per milliliter.

During the next steps monocytes were isolated from the gained PBMCs by magnetic-associated cell sorting. Four 50 ml tubes were prepared, with each tube containing 0.85 ml of the PBMC suspension. Then monocytes were magnetically labeled by adding 0.15 ml of a preparation of microbeads conjugated to anti-human CD14 monoclonal

antibodies to each tube. Subsequently the tubes were cooled at -20 °C for 15 min. After that the cells were washed with Hanks once and then resuspended in 2 ml Hanks per tube. MACS® cell separation columns were placed in a MACS® cell separator and equilibrated with Hanks. Then the content of each tube was applied to a column and the columns were washed with Hanks. Next, the columns with the retained labeled monocytes were removed from the magnetic field of the cell separator and the cells were eluted from the columns with Hanks. The resulting cell suspensions were pooled in a 15 ml tube and Hanks was added up to the 10 ml mark. The cell count of this suspension was determined using a Neubauer haemocytometer similarly as described above. After that the cell suspension was centrifuged for 10 min at 1214 rpm and decanted. The remaining cell pellet was suspended in RPMI medium for cells enriched with GM-CSF (100 $\frac{\mu g}{ml}$) and IL-4 (10 $\frac{\mu g}{ml}$) so that a cell concentration of 8.3×10^5 cells per milliliter was reached. Subsequently the cell suspension was distributed into 6-well plates with each well receiving 3 ml and therefore 2.5×10^6 monocytes.

In order to allow the differentiation of the monocytes into moDCs, the cells were cultured for five days after isolation. RPMI medium and the differentiation inducing cytokines GM-CSF and IL-4 were supplemented on day two and four after isolation. For that 1ml was taken from each well and replaced with 1 ml of RPMI medium containing GM-CSF and IL-4 at concentrations of 300 $\frac{\mu g}{ml}$ and 30 $\frac{\mu g}{ml}$, respectively. On the fifth day after isolation, the immature moDCs were ready to be harvested.

2.8. Cultivation and processing of *A. fum*

Conidia of *Aspergillus fumigatus* (*A. fum*) strain ATCC 46645 were obtained from the Institute for Hygiene and Microbiology, University of Würzburg and cultivated on beer mash agar plates for three days at 37 °C until the plates were densely covered with fungus. Then, endotoxin-free water was added and a cotton bud and a cell strainer were deployed to detach and singularize the conidia. The number of harvested conidia was determined with a Neubauer haemocytometer and the conidia were gently centrifuged and resuspended in sterile water resulting in a concentration of 2×10^8

conidia per milliliter. This suspension was stored at 4 °C and served as a source for all experiments involving the *A. fum* wild-type strain.

For the cultivation of *A. fum* germ tubes 0.5 ml of the conidia stock suspension were added to 20 ml of RPMI medium for fungus in a 50 ml tube, so that the conidia concentration approximated 5×10^6 conidia per milliliter. Subsequently this suspension was placed in a combined shaker-incubator device at 200 rpm and 37 °C. The growth of the fungus was regularly evaluated under the microscope. When the estimated average length of the germ tubes reached about 15 µm (usually after six to eight hours), the fungus was removed from the incubator and stored at 4 °C to be used as living germ tubes in an experiment on the following day.

The cultivation of *A. fum* hyphae required a longer period of incubation. Usually after ten to twelve hours in the shaker-incubator, the fungus showed long and branching filamentous growth and was regarded as *A. fum* hyphae.

For experiments with non-living fungal morphologies, the different growth stages were inactivated with ethanol. Conidia were taken from the stock conidia suspension and adjusted to a concentration of 5×10^6 conidia per milliliter in a total volume of 20 ml. Germ tubes and hyphae were directly processed after their cultivation. The tubes containing the different fungal morphologies were initially centrifuged and decanted. The pellets were then thoroughly suspended in 5 ml 70 % ethanol and stored at room temperature for 30 min. After that the fungal stages were washed with PBS twice and suspended in 1 ml RPMI medium 1640. Each milliliter was divided into portions of 200 µl and stored at -20 °C. The final concentration of fungal morphologies was 1×10^8 per milliliter based on the initial number of invested conidia. The success of the inactivation procedure was validated by cultivating samples of the inactivated fungal suspensions on malt extract agars.

2.9. Incubation of moDCs with different stimuli

Different groups of immature moDCs were either co-cultivated with living germ tubes of *A. fum* or cultivated in a medium containing various supposed stimuli, namely inactivated conidia, germ tubes or hyphae of *A. fum* wild-type, LPS, zymosan or

depleted zymosan. The cells were incubated with the stimuli for defined periods of time, i.e. one hour, two, four, six, nine and twelve hours. For each time point a group of moDCs was cultured in RPMI medium for cells without any potential stimuli as a negative control.

In detail, immature moDCs were harvested on the fifth day after their isolation as monocytes (see 2.7) with the help of a cell scraper. Each well was scraped a second time with a plastic pipette in 1 ml of Hanks. The empty wells were controlled for remnants of cells under a microscope and scraped again if needed. The cells were collected in 50 ml tubes and centrifuged at 1300 rpm for 7 min. Then the tubes were decanted and the cell pellets suspended in RPMI medium for cells. The cell count was determined with a Neubauer haemocytometer and the cell concentration was readjusted to 1 × 10^6 moDCs per milliliter by means of repeated centrifugation, decanting and resuspension of the cells in RPMI medium for cells. Usually the cell count amounted to circa a quarter of that of the originally seeded monocytes. GM-CSF and IL-4 were added to the medium so that their concentrations reached 100 $\frac{\mu g}{m卷}$ and 10 $\frac{\mu g}{ml}$, respectively. Portions of 1ml of this cell suspension (1 × 10^6 cells) were filled into 24-well plates and each well/unit of 1 × 10^6 cells was assigned to one specific stimulus and time point. The plates were put in the incubator until the stimuli were prepared.

Suspensions of *A. fum* wild-type and mutant germ tubes that had been generated the previous day (see 2.8) and stored over night at 4 °C, were readjusted to a concentration of 1 × 10^8 fungal stages per milliliter. In order to attain a multiplicity of infection (MOI) ratio of one, 10 µl of a suspension (containing 1 × 10^6 germ tubes) were given into a well with 1 × 10^6 immature moDCs.

Tubes with inactivated conidia, germ tubes and hyphae of *A. fum* at a concentration of 1 × 10^8 per milliliter (their preparation is described in chapter 2.8) were defrosted and 10 µl of each were added to different wells, resulting in a MOI of one. With inactivated germ tubes of *A. fum*, experiments were also conducted using MOIs of 2.5 and 5. For that, 25 µl (2.5 × 10^6 germ tubes) or 50µl (5 × 10^6 germ tubes) were added to a unit of 1 × 10^6 moDCs.

For the groups of moDCs being cultivated in a medium containing LPS, zymosan or depleted zymosan, concentrations of 1 $\frac{\mu g}{ml}$, 10 $\frac{\mu g}{ml}$ and again 10 $\frac{\mu g}{ml}$ were used for the respective stimuli.

The different stimuli were administered to the wells as synchronously as possible and the plates were subsequently moved into the incubator. The units of moDCs were taken out at their assigned time points, harvested into 1.5 ml tubes and directly processed for the isolation of miRNA miR-132, miR-146a and/or miR-155.

2.10. Isolation of RNA

Immediately after co-culture experiments, total RNA (including miRNA) was extracted using the *mir*Vana™ miRNA Isolation Kit, following the manufacturer's protocol. In detail, the samples of moDCs contained in 1.5 ml tubes were initially centrifuged for 5 min at 1300 rpm. The supernatants were then transferred to new tubes and stored at -20 °C for later usage (see 2.14). The remaining cells were washed with PBS and subsequently disrupted by adding 600 µl of Lysis/Binding Buffer. For organic extraction of RNA, $\frac{1}{10}$ volume (60 µl) of miRNA Homogenate Additive was given to each lysate. After vortexing, the tubes were left on ice for 10 min. Then 600 µl Acid-Phenol:Chloroform were added to each tube. The tubes were vortexed for 30 s and centrifuged for 5min at 10000 rpm. After that each tube showed three phases: an aqueous upper phase containing RNA, a compact interphase and a lower phase. The aqueous phases were carefully removed and transferred to fresh tubes. Subsequently, 1.25 volumes of 100 % ethanol were added to each tube. For each sample, a Filter Cartridge was placed into a Collection Tube and 700 µl of a sample were applied to one filter. In order to pass the mixture through the filter, the combined Filter Cartridges and Collection Tubes were then centrifuged for 15 s at 10000 rpm. The resulting flow-throughs were discarded and the rest of the samples were pipetted onto the Filter Cartridges. The centrifugation step was repeated and the flow-throughs were again discarded. After that, the filters were washed once with 700 µl Wash Solution 1 and twice with 500 µl Wash Solution 2/3. In each washing step, the wash solution was applied onto the filter, the sample was centrifuged and finally the flow-through was

discarded from the collection tube. In order to remove residual fluid from the filter, the filter tube assembly was centrifuged for 1 min at 10000 rpm. Subsequently, the Filter Cartridges were placed into new Collection tubes. 100 µl of pre-heated nuclease-free water were applied to the filters and the samples were centrifuged for 30 s at 10000 rpm to recover the RNA. The filters were then disposed and the Collection Tubes containing the RNA-eluates were stored at -20 °C.

To save time, cells harvested at time points 0 h and 1 h in the incubation experiment were processed up to the lysis step (adding of Lysis/Binding Solution) and kept in the refridgerator at 4 °C. Further steps were performed together with the samples of time point 2 h. Similarly samples of time points 4 h and 6 h, and 9 h and 12 h were processed together.

2.11. RNA concentration and purity

In advance of the reverse transcription step, the concentration and purity of the RNA samples were assessed by UV absorbance measurement. In preparation, the frozen RNA samples were thawed on ice and the spectrophotometer was blanked with water. 2 µl of a sample were applied to the spectrophotometer. The concentration of total RNA was calculated by

$$C\left(\frac{ng}{\mu l}\right) = \frac{1000 \times M}{\varepsilon \times l} \times A_{260},$$

where C is the concentration, l the path length, M the molecular weight, ε the extinction coefficient and A_{260} the absorbance at 260 nm. For total RNA, the term $\frac{1000 \times M}{\varepsilon \times l}$ approximates a value of 40 (Ambion 2011).

The purity of the RNA samples was assessed by comparing the absorbance at 230 nm, 260 nm and 280 nm. In harmony with the generally recommended acceptability criteria (Latham, 2010), samples with ratios of $\frac{A_{260}}{A_{230}}$ and $\frac{A_{260}}{A_{280}}$ ≥ 1.8 were regarded as acceptable.

2.12. Reverse transcription

The synthesis of single-stranded cDNA from total RNA samples was performed using the TaqMan® MiRNA Reverse Transcription Kit and sequence-specific reverse transcription primers from the TaqMan® MiRNA Assay series. That means each reverse transcription (RT) reaction was specific for a single miRNA, namely miR-132, miR-146a or miR-155.

Initially, each total RNA sample was diluted with nuclease-free water at a ratio of one to ten. After that the adjusted concentrations of total RNA in the samples usually ranged between 2.00 and 8.00 $\frac{ng}{\mu l}$. In order to normalize results, an equal amount of total RNA (10 ng) was taken from each sample and transferred to a RT reaction tube. To even up volumes, water was added so that each RT-reaction tube contained 5µl of total RNA solution at a concentration of 2 $\frac{ng}{\mu l}$. Subsequently, 7 µl of previously prepared RT master mix composed of 0.15 µl dNTP mix, 1.00 µl Multiscribe™ RT enzyme, 1.5 µl 10X RT Buffer, 0.19 µl RNase Inhibitor and nuclease-free water was added to each reaction tube. The tubes were mixed gently and centrifuged briefly. Finally 3 µl of the miRNA-specific RT primer were added. After short centrifugation, the tubes were placed in the thermal cycler, which was programmed as follows:

Step Type	Time (minutes)	Temperature (°C)
HOLD	30	16
HOLD	30	42
HOLD	5	85
HOLD	∞	4

Table 7

A negative control sample containing RNA and all master mix components except for the RT enzyme was always processed along.

After the RT step, the samples were directly processed further for polymerase chain reaction (PCR) amplification.

2.13. Polymerase chain reaction

Polymerase chain reaction (PCR) amplification of the cDNA samples was accomplished using the TaqMan® MiRNA Assay. Three PCR replicates for each cDNA sample were performed. For the negative control sample of the RT reaction only a single PCR reaction was performed and an additional negative control sample containing no cDNA input was added to each PCR plate.

In preparation of the PCR step, 18.67 µl of a PCR master mix were given to each well in the PCR reaction plate. The mentioned volume of the PCR master mix consisted of 10.00 µl TaqMan® 2X Universal PCR Master Mix, 7.67 µl nuclease free water and 1.00 µl TaqMan® MiRNA Assays 20X TaqMan® Assay. As recommended by the manufacturer, the RT reaction samples were diluted with water at a ratio of 1:15. Then 1.33 µl of the diluted RT product were added to the reaction wells. Consequently, the total volume of one reaction was 20 µl. After that, the PCR plate was sealed with an optical adhesive cover and briefly centrifuged. The plate was then placed in the real-time PCR system and run at the following thermal cycling parameters:

Step Type	Time	Temperature (°C)
HOLD	10 min	95
PCR CYCLE (40 cycles)	15 sec	95
	60 sec	60

Table 8

The results were exported from the real-time PCR system to a Microsoft® Excel file.

2.14. Data Analysis

Data analysis was performed in Excel using the $2^{-\Delta C'\mathrm{T}}$-method as described by Livak and Schmittgen (2001), calculating expression levels as fold-differences to the expression levels at time point 0 h or to unstimulated samples of the same time point.

As PCR amplification was carried out with three replicates for each sample, the arithmetical average of the three C_T values was used for further calculations. In order to calculate a fold-difference in expression level of a specific miRNA in a sample x

compared to a sample y (usually time point 0 h or unstimulated sample of the same time point), following formula was used:

$2^{-(CTx-CTy)}$

The result of this expression is the fold-difference by which the quantity of a specific miRNA is higher in sample x than in sample y. That means that if the result was 5, there would be five times as many molecules of a certain miRNA in sample x than in sample y.

This formula is based on the assumption that the quantity of target miRNA doubles with every PCR cycle, i.e. that PCR efficiency is 100 %. PCR efficiency was tested for this assumption (see Figure 8) and found to be adequate.

P-values were determined by a two-tailed paired Student's *t*-test. If the averaged C_T values at 0 h were 31.88, 29.11 and 30.37 in the three different donors for example, and the C_T values for a given stimulus and time point (say germ tubes at 9 h) were 28.55, 27.49 and 27.46 in the three donors, these two groups of C_T values made up the two samples of the *t*-test. With a resulting p-value of 0.04 in this example, it was concluded that the difference in the relative expression level of the miRNA was significant at a level of 0.04.

All experiments were conducted with material from at least three independent blood donors. A p-value of 0.01 or less was regarded as highly significant and corresponding results were marked with two asterisks (**). P-values above 0.01 up to and including 0.05 were described as significant (*).

2.15. ELISA from culture supernatants

The culture medium of each sample was recovered when a cell group was harvested during the incubation experiment and only the cells were further processed for miRNA isolation. In order to verify to what extent the relevant stimulus was able to activate the moDCs, the medium was analyzed for the contained quantity of IL-1β, Il-6 and CCL20 with Quantikine® ELISA Assays from R&D Systems® according to the manufacturer's protocol.

At first a medium-binding microplate was coated with the respective capture antibody by giving 100 µl of a 2 $\frac{\mu g}{ml}$ antibody preparation to each well. The plate was sealed and stored at room temperature over night. On the following day, the microplate was emptied out and blotted against clean paper toweling to eliminate air bubbles. Then 300 µl wash buffer were added to each well and the plate was put on a shaker for 30 s at 1000 rpm. After shaking, the washing buffer was thoroughly removed from the wells. This washing procedure was repeated three times. Subsequently, each well was blocked by applying 300 µl of blocking solution. After that, the plate was covered with an adhesive strip and incubated on the shaker for two hours at 600 rpm. The washing step was then repeated as described above. Subsequently, 100 µl standard buffer 1 were given to four wells for two positive and two negative control samples. 100 µl of previously prepared standard samples containing defined amounts of the specific chemokine were added to the appropriate wells. The chemokine concentrations of the eleven standard samples were 10, 5, 2.5, 1.25, 0.625, 0.313, 0.156, 0.078, 0.039, 0.0195 and 0.00975 $\frac{ng}{ml}$. The standard samples were prepared by step-wise dilution of the respective chemokine preparation in standard buffer 1. Similarly, 100 µl of each actual sample (medium from the incubation experiment) were transferred to the plate. Every sample was run in two replicates (two wells) in the ELISA assay. After sealing the plate, it was again incubated on the shaker for two hours at room temperature. Then the washing step was repeated as described previously and 100 µl of the detection antibody at a concentration of 4 $\frac{\mu g}{ml}$ were given to the wells with the standard samples and the actual samples. The control samples received 100 µl of standard buffer 2. The plate was sealed and incubated on the shaker for two hours at 600 rpm. After another washing step, 100 µl of Streptavidin-HRP were given to the samples and actual samples wells. 100 µl of standard buffer 3 was added to the wells containing the control samples. After sealing, the plate was placed on the shaker for 20 min at 600 rpm. After that, the washing step was repeated and 20 µl Streptavidin-HRP was applied to the wells with the positive control samples. Then, 100 µl of substrate solution were added to each well. The plate was sealed and was incubated protected from light at room temperature for 15 min. Subsequently 50 µl of stop solution were given to each well.

The optical density and thereby the concentration of the cytokine in question was then determined for each well with the help of a microplate reader set to 450 nm at a wavelength correction set to 570 nm.

3. Results

3.1. MiR-132 in DCs stimulated with living germ tubes of *A. fum* and LPS

In a first series of experiments, expression of miR-132, miR-146a and miR-155 was quantified in moDCs incubated with living germ tubes of *A. fum* or LPS. An untreated set of moDCs was kept as a negative control. MoDCs were harvested at different time points, namely after 0 h, 1 h, 2 h, 4 h, 6 h, 9 h and 12 h. It could be demonstrated that living germ tubes induce miR-132 expression in a time-dependent manner. The average induction fold was significantly elevated at 6 h, 9 h and 12 h when compared to samples at 0 h. Detailed data (including SEM and p-value) and their graphic illustration are given in Figure 1 and Table 9.

Ultrapure LPS caused no relevant changes in expression levels of miR-132 (Figure 1, Table 10).

As ultrapure LPS specifically stimulates the TLR4 pathway, it may be assumed, that in moDCs, miR-132 is not involved in the signaling cascade following TLR4 activation. *A. fum* however, additionally activates other pathogen receptors including TLR2, dectin 1 and DC-SIGN. In a previous study with monocytes from the THP-1 cell line, expression of miR-132 was linked to TLR2 activation (Nahid et al. 2013). Therefore, the ability of *A. fum* to induce miR-132 expression in moDCs, strongly suggests the involvement of miR-132 in the TLR2 pathway of DCs.

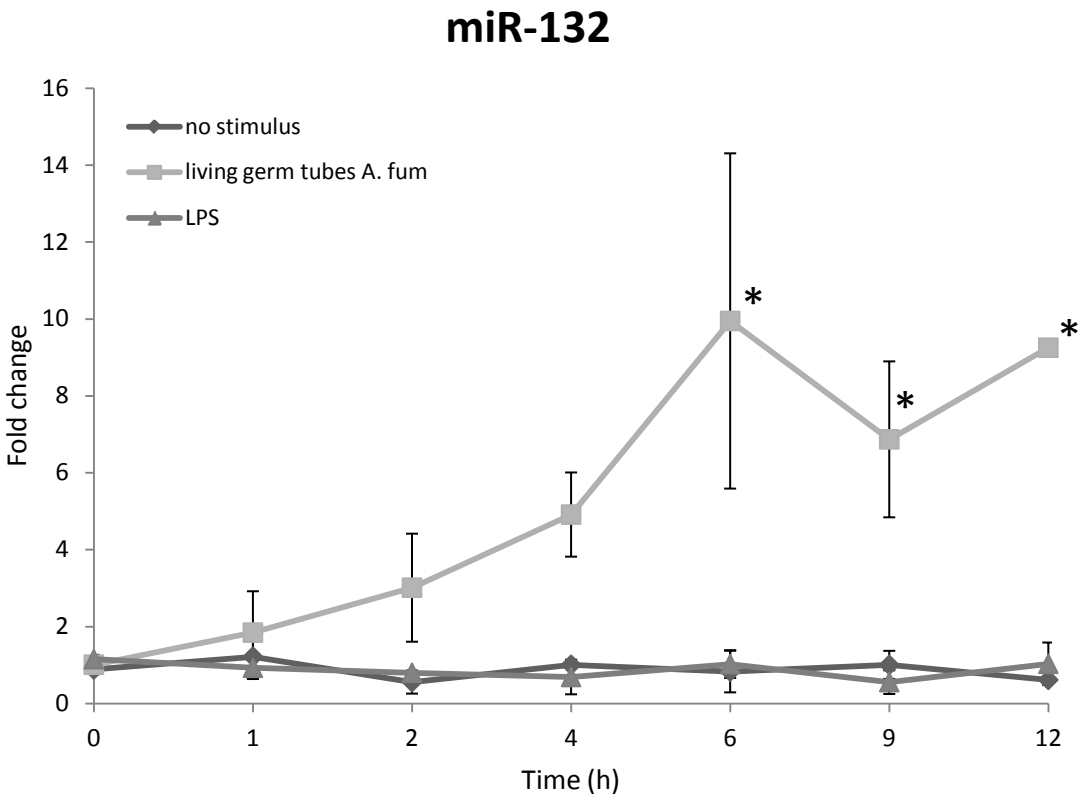

Figure 1. Expression kinetics of miR-132 in moDCs stimulated with living germ tubes of *A. fum* and LPS, analysed by RT-PCR. Data are presented as mean +/- SEM of three independent experiments. Significant results are marked with asterisks.

miR-132, living germ tubes of *A. fum*

	Compared to 0 h			
Time (h)	Induction fold	SD	SEM	p-value
1	1.84	1.86	1.07	0.87
2	3.01	1.99	1.40	0.13
4	4.91	1.55	1.09	0.07
6	9.95*	7.55	4.36	0.04
9	6.87*	3.51	2.03	0.04
12	9.25*	0.20	0.14	0.04

Table 9

miR-132, LPS

	Compared to 0 h			
Time (h)	Induction fold	SD	SEM	p-value
1	0.93	0.49	0.28	0.80
2	0.80	0.04	0.03	0.75
4	0.69	0.64	0.45	0.85
6	1.03	0.62	0.36	0.87
9	0.56	0.53	0.31	0.80
12	1.03	0.78	0.55	0.65

Table 10

3.2. MiR-146a in DCs stimulated with living germ tubes of *A. fum* and LPS

Analysis of miR-146a expression showed increased levels after LPS/TLR4 stimulation, but no changes after co-cultivation of DCs with living germ tubes of *A. fum*. The average expression fold values across the three donors are shown in Figure 2 and Table 11. MiR-146a expression in response to LPS peaked after 4 h of stimulation (5.32-fold increase), but even at peak level, the scale of up-regulation remained relatively low compared to miR-155 (51.81-fold increase). These results suggest that miR-146a is induced by activation of TLR4 (by LPS) but not via stimulation of TLR2, dectin-1 or DC-SIGN (by *A. fum*).

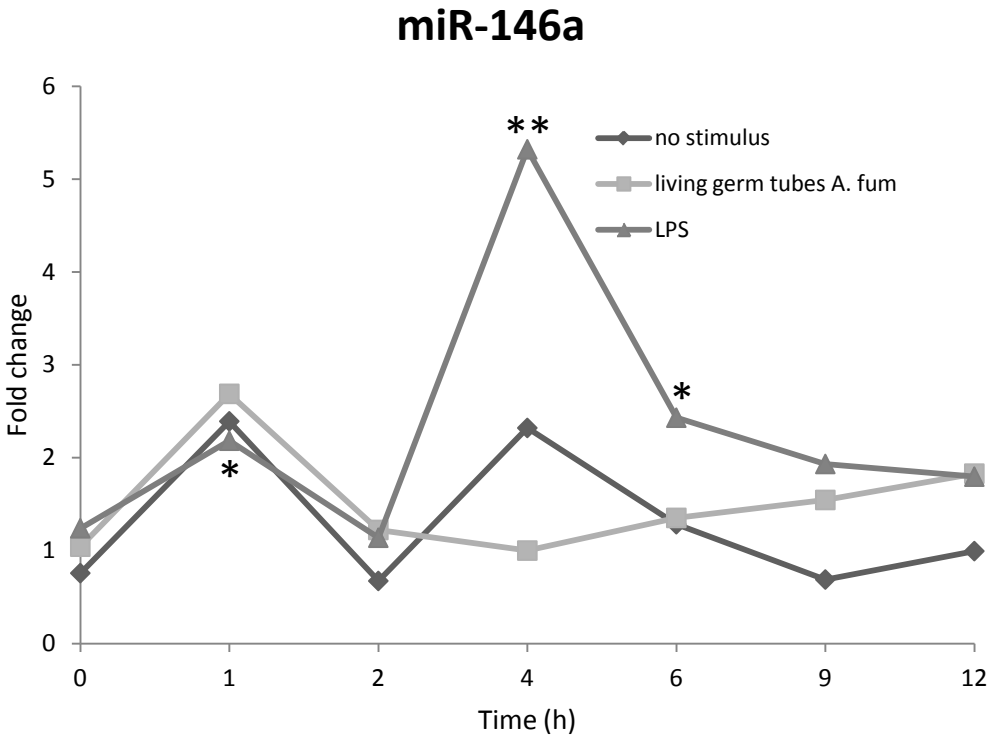

Figure 2. Expression kinetics of miR-146a in moDCs stimulated with living germ tubes of *A. fum* and LPS, analysed by RT-PCR. Data are presented as mean of three independent experiments. Significant results are marked with asterisks.

miR-146a

Compared to 0 h

	living germ tubes A. fum				**LPS**			
Time (h)	Induction fold	SD	SEM	p-value	Induction fold	SD	SEM	p-value
1	2,69	2,87	1,66	0,30	2,18	0,96	0,55	0,03
2	1,22	0,30	0,17	0,37	1,14	0,55	0,32	0,95
4	1,00	0,08	0,05	0,99	5,32**	2,88	1,66	0,01
6	1,35	0,59	0,34	0,32	2,43*	0,65	0,37	0,02
9	1,55	1,17	0,68	0,88	1,93	0,59	0,34	0,11
12	1,83	1,04	0,73	0,24	1,80	1,37	0,97	0,42

Table 11

3.3. MiR-155 in DCs stimulated with living germ tubes of *A. fum* and LPS

MoDCs displayed a strong time-dependent increase in the expression of miR-155 after stimulation with living germ tubes and LPS. When compared to the expression level at 0 h, living germ tubes induced a significant 3.46-fold increase at 4 h. Highly significant induction fold values of 9.50, 9.16 and 25.62 were seen after 6 h, 9 h and 12 h, respectively (see Figure 3 and Table 12). LPS proved to be an even stronger inductor of miR-155 with expression fold values up to 51.81 (see Figure 3 and Table 13).

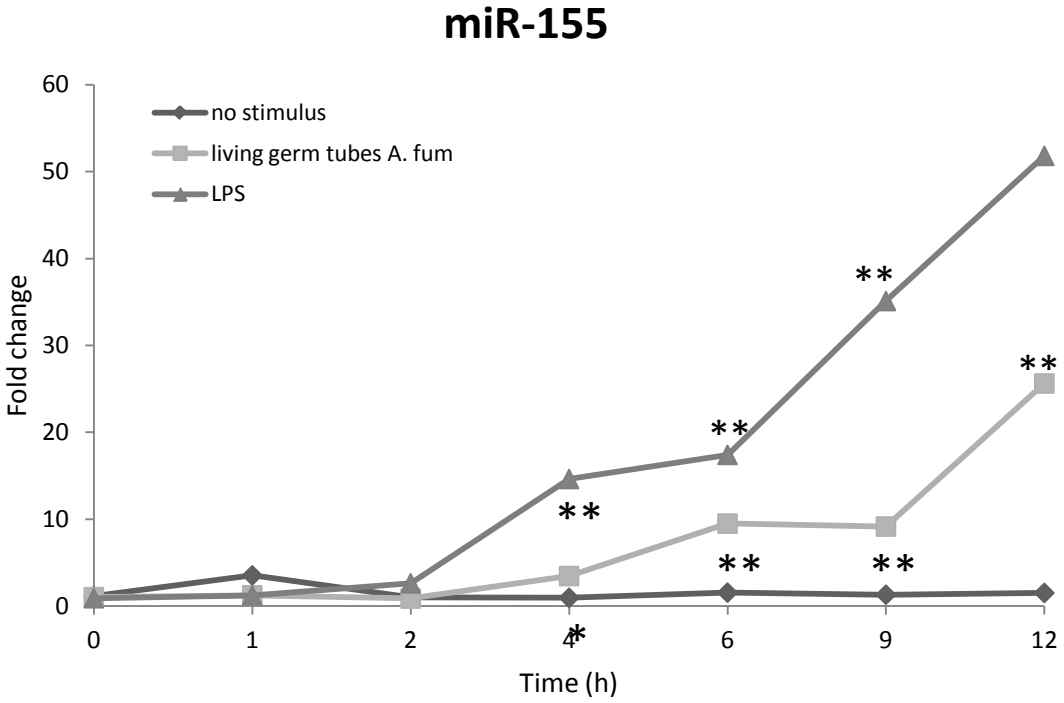

Figure 3. Expression kinetics of miR-155 in moDCs stimulated with living germ tubes of *A. fum* and LPS, analysed by RT-PCR. Data are presented as mean of three independent experiments. Significant results are marked with asterisks.

miR-155, living germ tubes of *A. fum*

	Compared to 0 h			
Time (h)	Induction fold	SD	SEM	p-value
1	1.25	0.44	0.26	0.39
2	0.88	0.64	0.37	0.51
4	3.46*	1.59	0.92	0.02
6	9.50**	3.56	2.06	0.00
9	9.16**	2.67	1.54	0.00
12	25.62**	3.63	2.56	0.00

Table 12

miR-155, LPS

	Compared to 0 h			
Time (h)	Induction fold	SD	SEM	p-value
1	1.24	0.34	0.20	0.28
2	2.63	1.98	1.15	0.26
4	14.63**	7.57	4.37	0.00
6	17.41**	9.40	5.43	0.00
9	35.11**	25.71	14.85	0.00
12	51.81	69.78	49.34	0.13

Table 13

3.4. MiR-155 in DCs stimulated with different morphologies of *A. fum*

Further experiments were performed with miR-155 only, as miR-155 expression was highest and most constant among the different blood donors. Besides, its expression was induced by both stimuli of the first experiment series, namely living germ tubes of *A. fum* and LPS. In order to evaluate the dependence of miR-155 expression on the morphology of *A. fum*, moDCs were incubated with inactivated conidia, germ tubes and hyphae for 4, 6 and 9 h. Groups of moDCs incubated with no stimulus or with LPS were processed along as negative and positive control samples. The experiments were again conducted with moDCs from three independent blood donors.

It could be shown that miR-155 induction was clearly influenced by fungal morphology. MoDCs stimulated with inactivated conidia of *A. fum* did not respond with a significant

change in miR-155 expression at any time point when compared to the expression level at 0 h. Inactivated germ tubes however, elicited a 3.62-fold increase at 6 h and a 9.09-fold increase at 9 h. For the inactivated hyphae groups, induction fold values reached 3.36 at 6 h and 5.02 at 9 h (see Figure 4 and Table 14).

In summary, miR-155 induction was lowest and insignificant with conidia, moderate with hyphae and highest with germ tubes of *A. fum*.

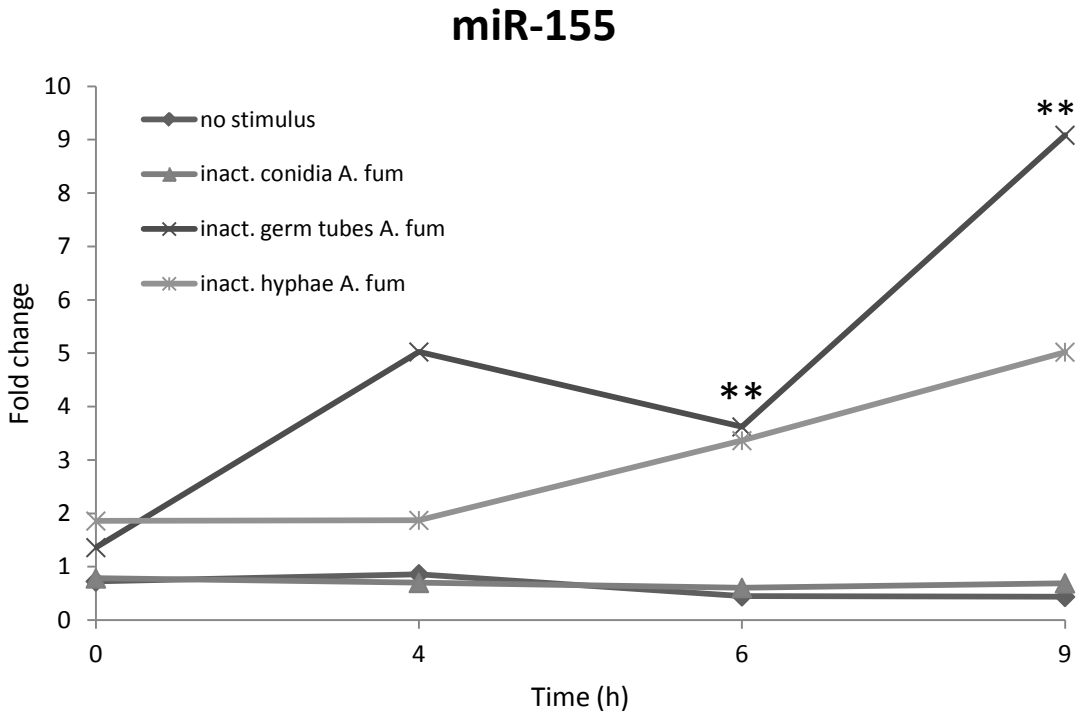

Figure 4. Expression kinetics of miR-155 in moDCs stimulated with inactivated condidia, germ tubes and hyphae of *A. fum*, analysed by RT-PCR. Data are presented as mean of three independent experiments. Significant results are marked with asterisks.

miR-155

	Compared to 0 h								
	inact. conidia *A. fum*			**inact. germ tubes *A. fum***			**inact. hyphae *A. fum***		
Time (h)	Induction fold	SEM	p-value	Induction fold	SEM	p-value	Induction fold	SEM	p-value
4	1.09	0.33	0.99	5.03	3.19	0.25	1.87	1.08	0.57
6	1.48	0.60	0.54	3.62**	0.74	0.00	3.36*	1.45	0.04
9	3.18	1.25	0.19	9.09**	2.56	0.00	5.02*	1.74	0.02

Table 14

3.5. MiR-155 in DCs stimulated with zymosan and depleted zymosan

Furthermore, it was analyzed wether zymosan (a ligand for TLR2 and dectin-1) and depleted zymosan (a ligand for dectin-1 only) are able to induce miR-155 expression. The experiments were carried out with moDCs from two different blood donors. Though statistically not significant, the results indicate that zymosan induced higher miR-155 expression levels than depleted zymosan after 4, 6 and 9 h, respectively (see Table 15 and Figure 5); expression levels increased by a factor of 4.64 in depleted zymosan samples and by 7.15 in zymosan samples after 9 h.

In view of this data, it may be asserted, that miR-155 is involved in the transduction pathways of both the TLR2 and the dectin-1 receptor.

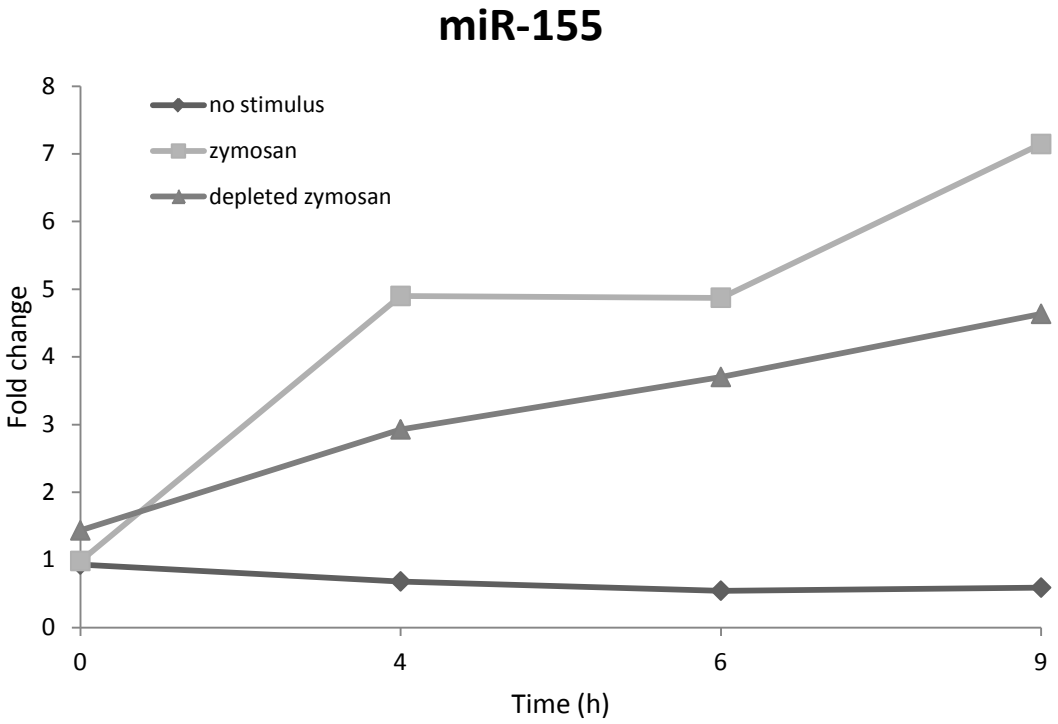

Figure 5. Expression kinetics of miR-155 in moDCs stimulated with inactivated zymosan and depleted zymosan, analysed by RT-PCR. Data are presented as mean of two independent experiments.

miR-155

Compared to 0 h

	depleted zymosan			**zymosan**		
Time (h)	Induction fold	SEM	p-value	Induction fold	SEM	p-value
4	2.93	0.94	0.33	4.90	2.39	0.28
6	3.70	1.13	0.25	4.87	1.06	0.16
9	4.64	0.13	0.11	7.15	1.62	0.11

Table 15

3.6. MiR-155 in DCs stimulated with germ tubes at different MOIs

In order to assess the effect of the multiplicity of infection on miR-155 expression, moDCs from three different blood donors were incubated with inactivated germ tubes of *A. fum* at fungus to cell ratios of 1:1, 2.5:1 and 5:1.

It was seen that a higher MOI regularly triggered stronger increases in miR-155 expression levels over time (see Figure 6 and Table 16).

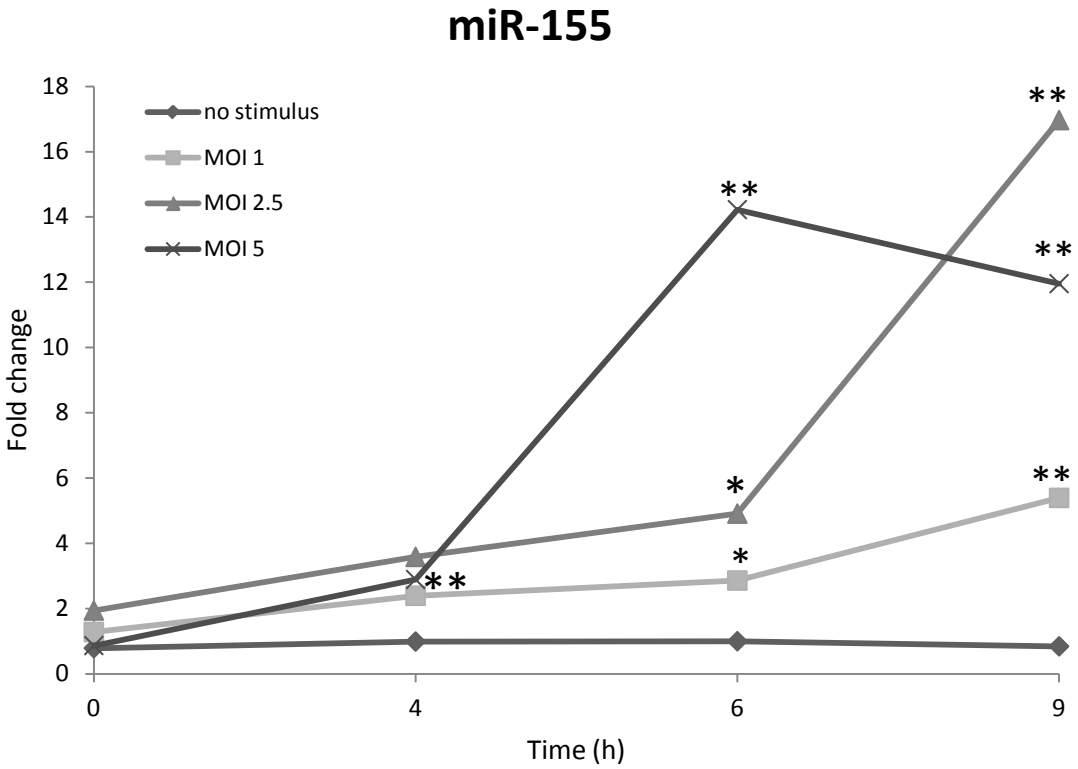

Figure 6. Expression kinetics of miR-155 in moDCs stimulated with inactivated germ tubes of *A. fum* at different MOIs, analysed by RT-PCR. Data are presented as mean of three independent experiments. Significant results have been marked with asterisks.

miR-155

Compared to 0 h, inact. germ tubes A. fum

	MOI 1			**MOI 2.5**			**MOI 5**		
Time (h)	Induction fold	SEM	p-value	Induction fold	SEM	p-value	Induction fold	SEM	p-value
4	2.39	1.28	0.38	3.58	1.51	0.09	2.89**	0.42	0.01
6	2.86*	0.89	0.03	4.91*	1.30	0.02	14.22**	9.22	0.01
9	5.39**	0.28	0.01	16.97**	3.17	0.01	11.95**	6.27	0.01

Table 16

3.7. Donor variability

Experiments were carried out with three biological replicates, i.e. with moDCs derived from the blood of three independent donors. Comparing the donors, a high variability in the magnitude of miRNA expression level change was observed. For example, donor number one displayed a relative miR-155 expression level of 10.25 at 9 h in response to LPS, whereas donor two reached a level of 33.48 and donor three a level of 61.60 (see Figure 7). Similar differences in the scale of miRNA induction were found in the experiments with miR-132 and miR-146a.

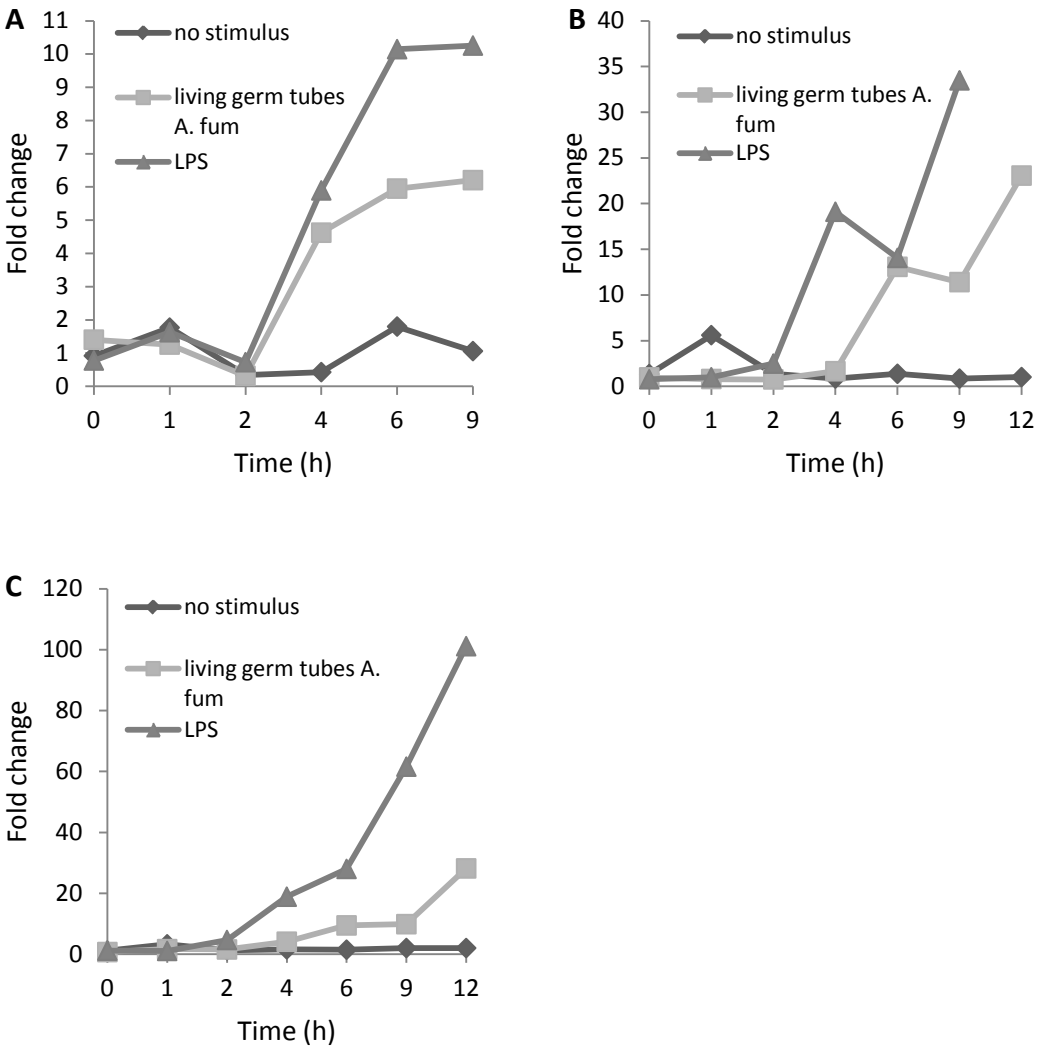

Figure 7. Expression kinetics of miR-155 in three different donors (A,B,C), analysed by RT-PCR.

3.8. PCR efficiency

The efficiency of the PCR experiment was evaluated with a dilution series. MiR-155 was used as a target. The RT-product was diluted with water at ratios of 1:3.75, 1:7.5, 1:15, 1:30, 1:60 and 1:120, i.e. for every dilution step, the miR-155 quantity was halved.

It was found that between dilutions of 1:15 and 1:120, a doubling of miR-155 quantity corresponded with a rise in C_T value by roughly 1 unit. Hence it was concluded that PCR efficiency was about 100% in this dilution range. For all experiments a dilution of 1:15 was used (see 2.13).

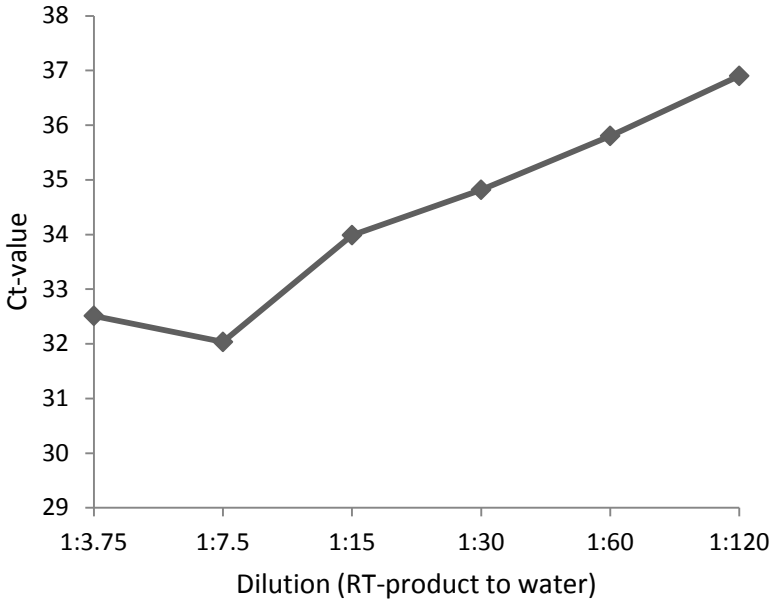

Figure 8. Dilution series of RT-product, determined by RT-PCR with miR-155 as target.

3.9. Cytokines in culture supernatants

In order to confirm that the applied stimuli were able to induce an inflammatory response, secretion of IL-1β, IL-6 and CCL20 was quantified. The mentioned cytokines were measured in culture supernatants collected from one incubation experiment with moDCs.

The secretion of IL-1β was most prominently induced by living germ tubes of *A. fum*, followed by LPS. Stimulation with inactivated conidia of *A. fum* did not lead to any secretion of IL-1β at all, whereas inactivated germ tubes and inactivated hyphae of *A. fum* resulted in moderate responses. Zymosan and depleted zymosan were equally able to elicit IL-1β production (see Figure 9).

Production of CCL 20 was almost equally high in DCs treated with LPS and living germ tubes of *A. fum*. Moderate secretions were induced by inactivated germ tubes, inactivated hyphae, zymosan and depleted zymosan. Induction by inactivated conidia remained low (see Figure 10).

Secretion of IL-6 was by far highest in DCs incubated with LPS. When comparing secretions induced by the other stimuli, the inactivated hyphae, living germ tubes, zymosan and depleted zymosan groups ranged on roughly the same level, whereas induction in the inactivated conidia and inactivated germ tubes samples lagged behind (see Figure 11).

In summary, LPS and living germ tubes of *A. fum* were found to be the most potent stimulators of cytokine production. Induction in the inactivated conidia samples was generally lower, and zymosan and depleted zymosan samples basically showed no differences.

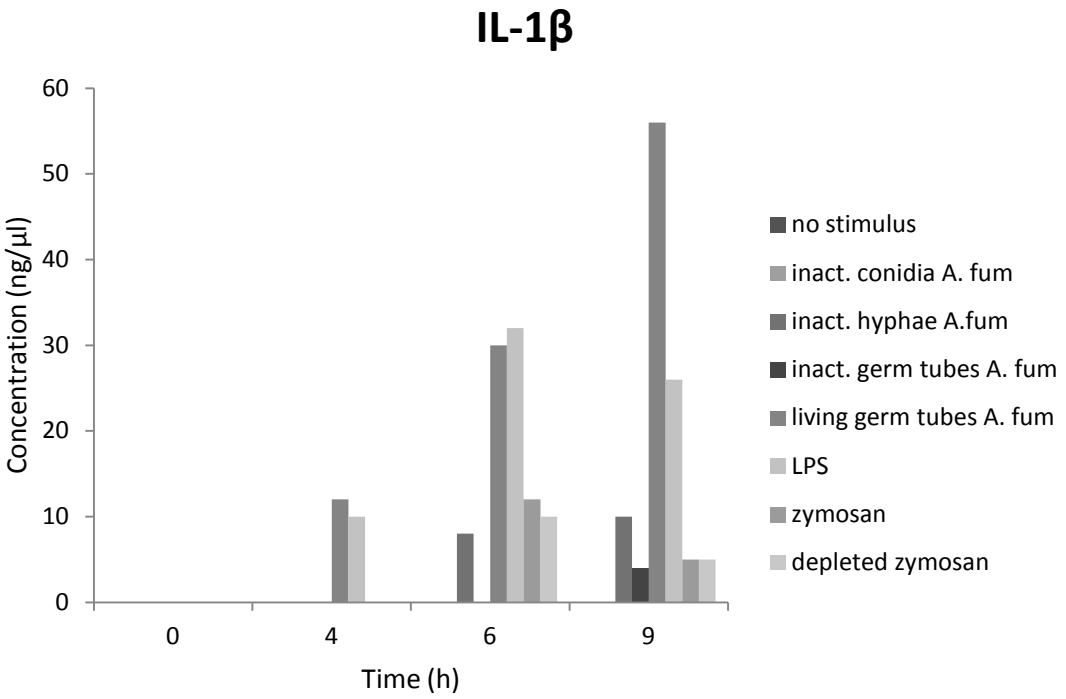

Figure 9. Expression of IL-1β in culture supernatant of stimulated moDCs measured by ELISA.

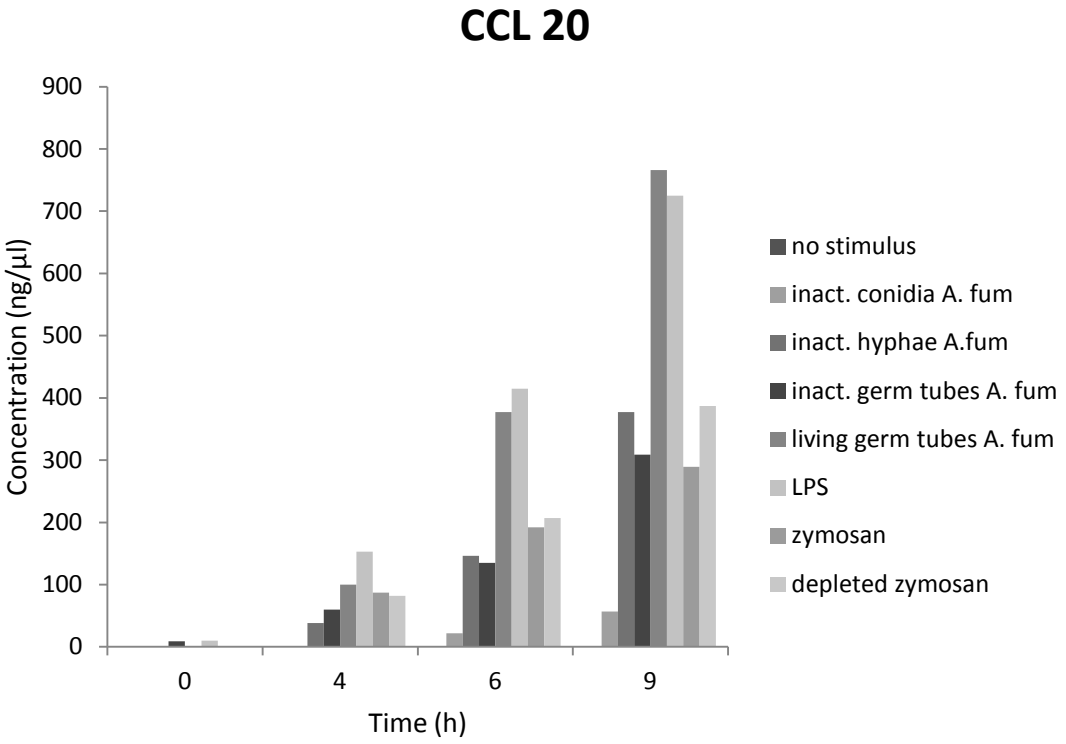

Figure 10. Expression of CCL 20 in culture supernatant of stimulated moDCs measured by ELISA.

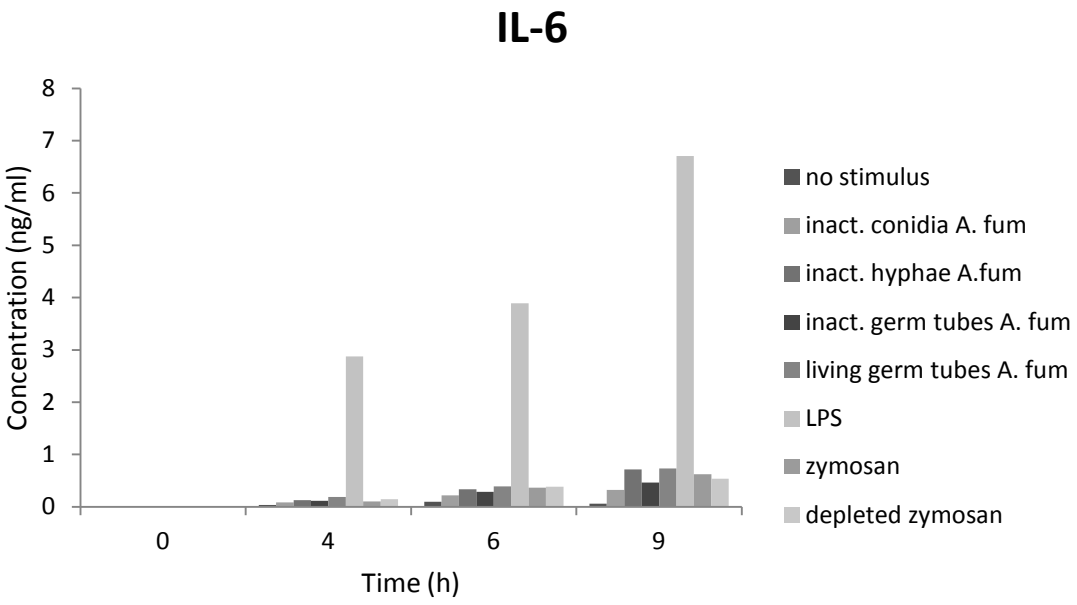

Figure 11. Expression of IL-6 in culture supernatant of stimulated moDCs measured by ELISA.

4. Discussion

4.1. MiRNA detection and expression profiling

Today, several methods for the detection and measurement of miRNA are available. Microarray analysis and deep sequencing allow the detection of different miRNAs in parallel, whereas real-time RT-PCR, Northern blotting and in situ hybridization (ISH) represent applications for the quantification of single miRNAs (van Rooij 2011).

Currently, Microarray analysis and real-time RT-PCR are the two methods most commonly used in miRNA profiling studies. Both approaches come with inherent advantages and limitations. Microarrays offer high throughput analysis of miRNA with a required amount of 100 – 10.000 ng RNA input, a limit of detection of 10^{-15} – 10^{-18} mol and a dynamic range of 10^{3} - 10^{4}. In comparison, throughput with the RT-PCR method is limited. The required amount of RNA is lower (10 – 700 ng) and sensitivity is higher with a detection limit of 10^{-22}. In addition, RT-PCR has a wider dynamic range of 10^{6} (Meyer et al. 2010). An issue that remains vital for both applications, is the adequate normalization of expression data. The appropriate approach for normalization of microarray data is subject to many recent studies (Hua et al. 2008; Pradervand et al. 2009; Sato et al. 2009; Git et al. 2010), however, no consensus on a certain approach has emerged yet.

In a RT-PCR experiment, expression levels can be normalized to an internal control gene. The main purpose is to account for different amounts of RNA added to the reverse transcription reactions (Livak and Schmittgen 2001). In addition, this method eliminates variations occurring during the RNA isolation procedure (Peltier and Latham 2008). Should the reverse transcription and PCR of the control and target gene be conducted in one tube, normalization to the internal control may also account for differing RT and PCR efficiencies. An important prerequisite to this method is, that the expression of the internal control gene is highly consistent, not altered by the experimental treatment and its amplification efficiency is the same as for the target gene. An alternative approach to using an internal reference gene, is to normalize expression values externally to the PCR experiment by determining the amount of RNA

added to the RT reaction by means of UV absorbance measurement (Livak and Schmittgen 2001).

When opting for an internal control gene in miRNA studies, it is ill-adviced to use traditional reference genes, such as GAPDH or β-actin, as due to their small size, miRNAs have different chemical properties. So far, the normalization of RT-PCR experiments with miRNA has generally been based on single reference genes such as 5S rRNA or the snRNAs U6, U24 or U26 (Peltier and Latham 2008; Mestdagh et al. 2009). However, Peltier et al. (2008) demonstrated that these commonly used normalizers show only insufficient expression stability across 13 normal and 5 pathological tissue types. The authors investigated the expression of 12 miRNAs and other small RNAs and used two different algorithms, geNorm and NormFinder, to assess the variance in expression levels. In normal human tissues, miR-191 and miR-93 were the most stable. The average standard deviation across all normal samples was lowest when expression levels were normalized to the geometric mean of miR-191 and miR-93. Next in rank were normalization to miR-191 alone and normalization to total RNA mass. The use of U6 and 5S lead to the highest standard deviations. Across five sets of cancer and normal adjacent tissue samples, miR-191 and miR-25 were most stably expressed. In tumor samples alone, miR-103 proved to be the most invariant RNA. The authors concluded that the stability of a given potential normalizer highly depended on sample type and handling. Therefore, a suitable miRNA normalizer should be experimentally selected for every new cell or tissue type (Peltier and Latham 2008). An approach to find appropriate normalizers in reduced scale experimental designs is described by Latham (2010). In an experimental setting that is intended to compare miRNA expression profiles between different sample groups, the author recommends to measure at least five potential reference candidates of miRNA in at least eight samples per group. The most stable candidate is then identified with the statistical program NormFinder. Potential reference candidate RNAs should be selected relying on existing publications. A universal method for miRNA RT-PCR data normalization is suggested by Mestdagh et al. (2009). The authors demonstrate that the mean expression value of all miRNAs expressed in given groups of samples serves

as the most accurate normalizer. This approach obviously requires the quantification of huge numbers of different miRNAs: Mestdagh et al. investigated the expression of at least 350 miRNAs per sample type. For small scale experiments, the authors advice the use of miRNAs that resemble the mean expression value, e.g. miR-572 and let-7f in normal tissue.

Many of the recent studies on miRNA expression in dendritic cells used non-validated normalizers. Chen et al. (2011a) and Zhang et al. (2011) for example arbitrarily chose U6 as a reference gene, Dunand-Sauthier et al. (2011) and Liu et al. (2010) used β-actin mRNA and Lu et al. (2011) opted for 5S RNA. Similar to the present study, Jansen et al. (2011) and Sun et al. (2011) normalized to total RNA input to the RT reaction. In combination to total RNA, they used let-7a and snoRNA135, respectively. These examples highlight the fact, that distinctive reference genes for miRNA profiling studies in DCs have yet to be established. As the scale of the present study precluded the validation of new reference genes, normalization to total RNA added to the RT reactions appeared to be the best choice. In respect to producing low standard deviations in expression values, this method ranked only third for normal tissues in the study of Peltier et al. (2008). The calculation of relative expression levels when normalizing to total RNA is conducted with the $2^{-\Delta C'\mathrm{T}}$ method (see 2.14). The derivations and applications of this method are described by Livak et al. (2001).

4.2. Effect of zymosan and LPS

Zymosan is a ligand for TLR2 and dectin-1, whereas depleted zymosan is a ligand for dectin-1 only (InvivoGen 2011a; InvivoGen 2011b). Interestingly, stimulation of moDCs with zymosan induced higher levels of miR-155 than depleted zymosan, emphasizing that parallel stimulation of both, TLR2 and dectin-1, lead to additive miR-155 levels. However, there was no difference in the level of secreted cytokines between DCs stimulated with zymosan and DCs stimulated with depleted zymosan, showing that both stimuli are equally capable of inducing DC maturation.

As an ultra pure LPS preparation, which only activates TLR4, was used in this study, induction of miRNAs by LPS was mediated by this receptor only. Other LPS preparations may contain lipoproteins that also activate TLR2.

4.3. Different morphologies of *A. fum*

Compared to inactivated conidia and inactivated hyphae, inactivated germlings of *A. fum* provoked maximal levels of miR-155. Accordingly, secretion of inflammatory cytokines was lower in the DCs samples treated with inactivated conidia. These observations are congruent with former studies that have shown the time/morphology-dependent differential expression or presentation of immune relevant genes in *A. fum* and their recognition by innate immunity. In resting conidia, β-glucan, the fungal cell wall component that ligates dectin-1 on immune cells, is masked by an external layer of immunologically inert hydrophobins composed of RodA protein. Thus, β-glucan is shielded away from recognition by innate immune cells. Only upon swelling, the rodlet layer is lost and β-glucan is displayed (Aimanianda et al. 2009). Equally, the TLR pathway is not activated by dormant conidia. Activation only starts to occur during conidial swelling (Hohl et al. 2005). Another phenotypic switch takes place during the germination into hyphae, resulting in a loss of TLR4 signaling in responding immune cells (Netea et al. 2003).

4.4. MiRNA profiles in monocytes and DCs

A number of recent studies shed light on the miRNA expression in monocytes and dendritic cells.

In addition to profiling miR-132, miR-146a and miR-155 in DCs, our group also investigated the expression of miR-132 and miR-155 at 2, 4 and 6 h in monocytes challenged with LPS and different morphologies of *A. fum*. Similar to DCs, miR-132 expression in monocytes was not altered by LPS/TLR4 stimulation, whereas co-cultivation with *A. fum* resulted in higher levels of miR-132. Stimulation with LPS also led to an increase in miR-155, however, unlike moDCs, monocytes did not respond with an increased expression of miR-155 to co-cultivation with *A. fum* (unpublished data from our group by Hannes Schloßnagel and Tanja Breitschopf).

In an extensive study by Jansen et al. (2011), monocytes, immature DCs (iDCs) and three mature DC subsets were screened for the expression of 157 different miRNAs. The mature DC subsets consisted of classic mature DCs (mDCs) that had been stimulated with LPS, tolerogenic DCs (tDCs) generated by stimulation with IL-10 and dexamethasone and activated tolerogenic DCs (atDCs), which comprise tDCs additionally stimulated with LPS. 104 of the 157 tested miRNAs were detected in monocytes and/or DCs. 18 miRNAs showed a differential expression pattern when comparing monocytes, all DCs and DC subsets. In accordance with the results of our group, relative expression of miR-155 was low in unstimulated monocytes, higher in immature DCs and markedly up-regulated in mature DCs, i.e. upon maturation induced by LPS. Jansen et al. postulate, that miR-155 is differentially expressed in monocytes and DCs, and that miR-155 is part of the TLR4 mediated response to LPS. The results of the present study not only confirm the role of miR-155 in the TLR4 mediated maturation of DCs induced by LPS, but also demonstrate that maturation induced by different morphologies of *A. fum*, zymosan or depleted zymosan is also accompanied with an increased miR-155 expression. Therefore, the up-regulation of miR-155 in maturating DCs is not specific for the LPS/TLR4 pathway, but may also be part of the TLR2, dectin-1 and/or DC-SIGN signaling cascades. The characterization of miR-146a expression by Jansen et al. yielded similar results to the miR-155 expression pattern. MiR-146a expression was up-regulated in mature DCs. As in the study of Jansen et al. maturation of DCs was achieved by stimulation with LPS for 6 h, this finding is consistent with the present study which revealed a significant 2.43* increase for the same time span and stimulus.

A publication by Tserel et al. (2011) states that out of 380 miRNAs, detected in monocytes, dendritic cells and macrophages, 49 miRNAs showed differential expression depending on the cell type. When immature DCs were incubated with LPS or curdlan (a dectin-1 ligand) for 6 h, they reacted with an elevated expression of miR-155, a result that is consistent with the current study. Tserel et al. also reported the same behavior for miR-146a. As said above, the induction of miR-146a by LPS is supported by our study, however, the stimulation of DCs with living germ tubes of *A.*

fum, a stimulus that is expected to ligate dectin-1, showed no significant results in respect to miR-146a levels. Moreover, Tserel et al. demonstrate that miR-132 expression in DCs is not influenced by LPS or curdlan stimulation, but is mainly induced during the differentiation phase from monocytes to moDCs. Again, this is compatible with our results, where miR-132 in DCs was not induced by LPS. However, miR-132 was induced by living germ tubes of *A. fum*. Considering the failure of curdlan to produce a miR-132 induction as reported by Tserel et al., the up-regulation of miR-132 by *A. fum* in this study might have been independent of dectin-1 signaling.

A specific study on miR-155 expression in DCs was conducted by Dunand-Sauthier et al. (2011). In a preliminary experiment, the authors verified that among a large number of tested miRNAs, miR-155 was the most strongly and reproducibly expressed in maturing DCs stimulated with LPS. Time-course experiments revealed a progressive increase in miR-155 levels with a maximum after 24-48 h. When maturation was induced by poly (I:C) (a TLR3 ligand), PGN (a TLR2 ligand), flagellin (a TLR5 ligand) or TNF-α, miR-155 was up-regulated in a similar manner, although the effect was weaker than that observed for LPS. These results correspond with the findings of the present study and underline the role of miR-155 up-regulation during DC maturation. The maturation induced expression of miR-155 appears to be a conserved process, as Dunand-Sauthier et al. confirm the above results in mouse DCs. Furthermore, DCs from miR-155 knock-out mice exhibited limited maturational and functional capacities, a finding that indicates the requirement of miR-155 for these processes. Dunand-Sauthier et al. present evidence, that miR-155 acquires its importance in DCs by silencing the expression of the transcription factor c-fos. So far, c-fos has been implicated in all kinds of different biological processes and its definite role in DCs remains to be elucidated (Dunand-Sauthier et al. 2011).

A study by Lu et al. (2011) grants further insight to miRNA profiles of dendritic cells. The authors identified 15 miRNAs that were decreased and 12 miRNAs that were increased during monocyte differentiation into DCs. When immature and mature DCs were compared, miR-155 was one of the two miRNAs that were markedly up-

regulated. MiR-146a was found to be slightly increased in mature DCs. On the basis of further experiments, the authors established KPC1, a gene that is involved in cell cycle and apoptosis regulation, as a target of miR-155. They revealed, that over-expression of miR-155 leads apoptosis of immature DCs. Over-expression of miR-155 had another effect in mature DCs, namely secretion of higher levels of IL-12p70.

Two publications by Chen et al. (2011a; 2011b) further illuminate the role of miR-146a and miR-155 in dendritic cells. Both miR-146a and miR-155 were up-regulated in DCs when maturation was induced by oxidized low density lipoprotein (oxLDL). On the basis of various experiments, the authors postulate that miR-146a regulates the maturation process and cytokine response of oxLDL stimulated DCs by directly targeting CD40L (Chen et al. 2011a). MiR-155 is suggested to regulate lipid uptake and SCG2 (secretory granin 2) expression in the same cell type. SCG2 is associated with various diseases, e.g. amyotrophic lateral sclerosis (Chen et al. 2011b).

The group of Martinez-Nunez et al. (2009) report that the expression of DC-SIGN in DCs is modulated by miR-155. Initially, the authors demonstrate an increase in miR-155 expression in DCs stimulated with LPS, a finding that is consistent with our data. They furthermore prove that miR-155 directly targets the transcription factor PU.1 which results in decreased mRNA and protein levels of DC-SIGN. In consequence, DCs with inhibited miR-155 function exhibited an enhanced binding capacity for Candida albicans and the HIV-1 protein gp120.

Ceppi et al. (2009) report a further investigation on miR-155 and miR-146a in moDCs. Consistent with our findings, they demonstrate that both miRNAs are up-regulated upon maturation induced by LPS, albeit miR-146a to a lesser degree than miR-155. The authors identified several pathways influenced by miR-155 in maturating DCs, e.g. the TLR/IL-1 signaling pathway and the mitogen-activated protein kinase p38 (p38 MAPK) pathway, a signaling cascade involved in cellular responses to injury and inflammation. TAB2, a protein involved in the TLR/IL-1 pathway, was established as a direct target of miR-155. It was further demonstrated that various inflammatory cytokines were regulated by miR-155.

In a study on miRNA profiles in plasmacytoid dendritic cells (pDCs), Zhou et al. (2010) discovered that 19 miRNAs altered their expression level when maturation of PDCs was induced by a TLR7 ligand. Further experiments revealed, that the highest induced miRNAs, miR-155 and its complementary partner miR-155*, were induced by TLR7 through the c-Jun N-terminal kinase pathway. Secretion of IFN-α and IFN-β were promoted by miR-155* and impaired by miR-155. The authors identify a target linked to interferon production for each of the two miRNAs and conclude that miR-155 and miR-155* cooperatively regulate interferon production by PDCs.

For studies dealing with miRNAs other than miR-132, miR-146a and miR-155 in DCs, please refer to Hashimi et al. (2009), Liu et al. (2010), Sun et al. (2011), Zhang et al. (2011) and others.

4.5. MiR-132 in the immune system

Compared to miR-155 and miR-146a, studies on miR-132 in the immune system are rare so far. Two already cited publications report that miR-132 is up-regulated in THP-1 cells after stimulation with LPS (Taganov et al. 2006; Nahid et al. 2011). The present study does not confirm this observation for moDCs, as miR-132 expression was only induced by living germ tubes of *A. fum* and not by LPS. In a recent study with THP-1 cells, miR-132 was induced by LPS/TLR4, PGN/TLR2 and flagellin/TLR5 stimulation. Activation of the TLR3 pathway with poly (I:C) did not affect miR-132 expression. It was further shown that within the TLR2 pathway, the expression of miR-132 (and also miR-212) was dependent on the transcription factor CREB. Additionally, IRAK4, a pivotal adaptor kinase for all TLR except TLR3, was identified as a target of miR-132. Based on this, expression of miR-132 is supposed to constitute a negative feedback mechanism in order to attenuate TLR response (Nahid et al. 2013).

In an interesting study on the involvement of miR-132 in the brain-immune axis, it was demonstrated that miR-132 is responsible for an anti-inflammatory effect by targeting acetylcholinesterase in murine brain tissue (Shaked et al. 2009).

4.6. MiR-146a in the immune system

Together with miR-146b, miR-146a belongs to the miR-146 miRNA family. Although the two miRNAs differ by only two nucleotides in their mature sequence, their loci are found on separate chromosomes in quite unrelated sequence contexts (Williams et al. 2008; Boldin et al. 2011). In experiments with cells of the acute monocytic leukemia (THP-1) cell line, miR-146a was induced to a different extent by stimulation with TNF-α, IL-1β and of TLRs that reside on the cell surface (TLR2, TLR4, TLR5), but not by stimulation of intracellular TLRs (TLR3, TLR7, TLR9). Promoter analysis revealed that miR-146a responsiveness to LPS is completely dependent on binding sites of the transcription factor NF-κB. On the basis of further investigations, IL-1 receptor associated kinase (IRAK1) and TNF receptor-associated factor 6 (TRAF6) were identified as direct targets of miR-146a (Taganov et al. 2006). IRAK1 and TRAF6 represent key proteins in the TLR and IL-1 receptor signaling cascades which lead to the activation of transcription factor NF-κB and AP-1. In view of this results, Taganov et al. postulate a negative feedback mechanism, wherein miR-146a is induced by bacterial components via the TLR/IRAK1/TRAF6/NF-κB pathway, and once expressed, inhibits the same pathway. The role of IRAK1 and TRAF6 as targets of miR-146a is supported by another publication of the same study group (Boldin et al. 2011). In this publication, the authors further describe the function of miR-146a in various immune cells on the basis of experiments with miR-146a mutant mice. In accordance with the previously proposed negative feedback mechanism, cells from miR-146a-null mice were found to be hypersensitive to LPS and miR-146a over-expression lead to a dampened inflammatory response. The function of miR-146a as a negative feedback regulator of NF-κB activation was also evaluated by Zhao et al. (2011). The authors demonstrate, that miR-146a deficient mice develop myeloid malignancies fully attributable to the dysregulation of NF-κB. Further proof for the mentioned feedback mechanism is given by Nahid et al. (2011): Inhibition of miR-146a in THP-1 cells produced markedly higher levels of IRAK1 and TRAF6 and entailed an increased TNF-α production. Besides, miR-146a was shown to mediate homologous tolerance and cross-tolerance of TLR signaling in THP-1 cells. These terms describe the phenomenon that cells primed with a

certain TLR stimulus, in this case LPS, exhibit a state of hyporesponsiveness to following stimulation with the same or other TLR ligands. The introduction of miR-146a mimics alone is able to induce this tolerance in THP-1 cells, comparable to the effect of LPS priming.

Lu et al. (2009) report, that miR-146a has a pivotal function for regulatory T cells (Treg). The effect of miR-146a on Treg cell function was ascribed to the direct targeting of signal transducer and activator of transcription 1 (STAT1) in Treg cells. In mice, inhibition of miR-146a lead to dysregulated IFNγ responses by Th1 due to impaired Treg function, which ultimately resulted in immune-mediated lesions in various organs.

The inflammatory response of human lung alveolar epithelial cells upon stimulation with IL-1β was also reported to involve miR-146a. By over-expression and inhibition of miR-146a, the miRNA was shown to reciprocally regulate IL-8 and RANTES (= CCL5) secretion in this cell type (Perry et al. 2008).

The expression of miR-146a was also subject to studies focusing on autoimmune diseases, defining a role for miR-146a in rheumatic arthritis, systemic lupus erythematodes and psoriasis (Li et al. 2010).

4.7. MiR-155 in the immune system

Among other miRNAs, miR-155 and miR-146a have been assigned outstanding roles in immune processes (Taganov et al. 2007; Lindsay 2008; Tsitsiou and Lindsay 2009; Xiao and Rajewsky 2009; O'Connell et al. 2010b).

Within the genome, miR-155 is located within the noncoding B cell integration cluster (BIC) gene, which was first identified as a common integration site for the avian leukosis virus in B cell lymphomas (Lagos-Quintana et al. 2001). In order to illuminate the role of BIC/miR-155 in the immune system, Rodriguez et al. (2007) tested the function of T cells, B cells and DCs derived from BIC deficient mice. All three cell types showed altered phenotypes and functional impairment. Expression of MHCII and cytokine secretion by DCs appeared normal, however, T cell stimulation by DCs was highly defective. In Th2, cMaf, a transactivator of the IL-4 promotor, was found to be a

direct target of miR-155. In general, BIC deficient mice showed marked remodeling of lung airways, suffered from enteric inflammation and failed to respond to vaccination. With special attention on B cells in a combined genetic-loss and gain-of-function approach of miR-155/BIC in mice, Thai et al. (2007) furthermore demonstrated that miR-155 is involved in the regulation of the germinal center response. The described effect was partly attributed to the regulation of cytokine levels by miR-155 and to altered T cell function. Vigorito et al. (2007) confirmed the role of miR-155 for proper B cell function. Additionally, the authors postulate that miR-155 regulates the terminal differentiation program of B cells into plasma cells, with PU. 1, a member of the Ets domain-transcription factor family involved in hematopoiesis, as one of the direct targets. As further primary targets, SHIP1, an inositol phosphatase associated with tumor growth and SOCS1, suppressor of cytokine signaling 1, were identified (Lu et al. 2009; O'Connell et al. 2009; Pedersen et al. 2009; Wang et al. 2010). In regulatory T cells, miR-155 expression appeared to be dependent on Foxp3, a X chromosome-encoded transcription factor that plays a vital role for the function of this cell type (Lu et al. 2009). A study on miR-155 in macrophages revealed that expression of miR-155 is mediated by the JNK (c-Jun N-terminal Kinase) pathway or pathways that are dependent on MyD88 or TRIF, both key adaptor molecules of the TLR signaling cascade (O'Connell et al. 2007). Finally, a recently published investigation establishes miR-155 as a player in autoimmune inflammation. O'Connell et al. (2010a) show that miR-155 deficient mice are resistant to experimental autoimmune encephalomyelitis, which is attributable to an altered development of inflammatory T cells.

5. Summary

The field of microRNA research has gained enormous significance during recent years. Current studies have shown that microRNAs play an important role in many biological processes via posttranscriptional gene regulation. This also applies for the TLR-mediated recognition of pathogens by immune cells. Among others, the microRNAs miR-132, miR-146a and miR-155 have been characterized by various authors. However, the specific role of microRNAs in the defense against fungal infections by *Aspergillus fumigatus* has not been investigated so far, although this ubiquitous mold causes severe infections in immuno-compromised patients. As dendritic cells play a pivotal part in the *in vivo* recognition of *A. fumigatus*, the present study investigates the reaction of these cells to *A. fumigatus* and other pathogens on the microRNA level. For this purpose, dendritic cells were incubated with different forms of *A. fumigatus* and other pathogens for up to twelve hours. Subsequently, the expression of miR-132, miR-146a and miR-155 was quantified by real-time PCR.

Levels of miR-132 in dendritic cells were significantly increased after stimulation with living germ tubes of *A. fum*, but showed no change after treatment with LPS. Relative expression level of miR-146a was moderately elevated upon stimulation with LPS, but did not respond to co-cultivation with living germ tubes. MiR-155 was highly induced by both stimuli. These results show, that dependent on the stimulus, microRNAs are differentially regulated in dendritic cells. Among the tested microRNAs, miR-155 showed the strongest and most stable expression values. Therefore, further experiments focused on this mircoRNA. It was shown, that the up-regulation of miR-155 is dependent on the germination stage of the fungus. Induction of miR-155 was low with conidia, moderate with hyphae and high with germ tubes. The extent of miR-155 induction also corresponded with the *multiplicity of infection* (MOI), with higher MOIs triggering a stronger miR-155 response.

These results suggest that miR-132 and miR-155 play an important role in the immunologic reaction of DCs against *A. fumigatus* and that a further characterization

of these microRNA, especially with respect to their specific function in DCs, could contribute to the understanding of the biological mechanisms of Aspergillosis.

Zusammenfassung

Die Erforschung von MicroRNAs gewinnt zunehmend an Bedeutung. Aktuelle Arbeiten zeigen, dass MicroRNAs an der Regulation vieler biologischer Prozesse beteiligt sind, indem sie in die posttranskriptionelle Genregulation eingreifen. Dies betrifft auch die TLR-vermittelte Erkennung von Pathogenen durch Immunzellen. Hierbei wurden u.a. die MikroRNAs miR-132, miR-146a und miR-155 von verschiedenen Autoren charakterisiert. Die spezielle Rolle von MikroRNAs bei der Abwehr von Pilzinfektionen durch *Aspergillus fumigatus* ist bisher allerdings kaum untersucht, obwohl dieser ubiquitär vorkommende Schimmelpilz häufig schwere Infektionen bei immunsupprimierten Patienten auslöst. Da *in vivo* den dendritischen Zellen eine entscheidende Rolle bei der Erkennung von *A. fumigatus* zukommt, wurde in der vorliegenden Arbeit die Reaktion dieser Zellen auf *A. fumigatus* und andere Pathogene auf MikroRNA Ebene untersucht. Dazu wurden dendritische Zellen mit verschiedenen Formen von *A. fumigatus* und LPS über Zeiträume von bis zu zwölf Stunden stimuliert. Anschließend wurde die Expression von miR-132, miR-146a und miR-155 mittels Real-Time PCR bestimmt.

Dabei zeigte sich, dass nach Stimulation mit *A. fumigatus* die miR-132 Level in dendritischen Zellen deutlich anstiegen, wohingegen eine Inkubation mit LPS keinen Einfluss auf diese MicroRNA hatte. Die relative Expression von miR-146a war nach Stimulation mit LPS leicht erhöht, zeigte allerdings keine Veränderung nach Ko-Kultur mit *A. fumigatus.* Die Expression von miR-155 wurde durch beide Stimuli stark induziert. Diese Ergebnisse zeigen, dass abhängig vom Stimulus eine differentielle Expression von MicroRNAs in dendritischen Zellen stattfindet. Unter den drei untersuchten MicroRNAs, zeigte miR-155 die höchsten und stabilsten Expressionswerte. Daher wurde der Schwerpunkt weiterer Experimente auf diese MicroRNA gesetzt. Dabei ergab sich, dass das Ausmaß der miR-155 Induktion vom Entwicklungsstadium des Pilzes abhängig ist. Konidien von *A. fumigatus* führten

lediglich zu einer schwachen Hochregulation von miR-155, wohingegen Hyphen und insbesondere Keimschläuche ein starke Induktion von miR-155 verursachten. Die Dynamik der miR-155 Hochregulation korrelierte außerdem mit der *multiplicity of infection* (MOI), wobei eine höhere MOI mit einer stärkeren miR-155 Antwort einherging.

Die dargestellten Ergebnisse legen nahe, dass miR-132 und miR-155 eine wichtige Rolle bei der Immunreaktion von DCs gegen *A. fumigatus* spielen und eine weitere Charakterisierung dieser MicroRNAs v.a. im Hinblick auf ihre spezielle Funktion in DCs einen wichtigen Beitrag zum Verständnis der biologischen Grundlagen der Aspergillosen erbringen könnte.

6. Appendix

6.1. Abbreviations

Abbreviation	Meaning
rpm	rounds per minute
MOI	multiplicity of infection
SEM	standard error of the mean
SD	standard deviation
nt	nucleotide(s)
3' UTR	3' untranslated region
A. fum	*Aspergillus fumigatus*
RISC	RNA-induced silencing complex
LNA	locked nucleic acid
IA	invasive aspergillosis
IFIs	Invasive fungal infections
HSCT	hematopoietic stem cell transplantation
SOT	solid organ transplant
GVHD	graft versus host disease

Abbreviation	Meaning
EORTC/MSG Consensus Group	European Organization for Research and Treatment of Cancer/Invasive Fungal Infections Cooperative Group and the National Institute of Allergy and Infectious Diseases Mycoses Study Group Consensus Group
AML	acute myeloid leukemia
MDS	myolodysplastic syndrome
IFD	invasive fungal disease
IDSA	Infectious Disease Society of America
PMNL	polymorphonuclear leucocyte
ROI	reactive oxygen intermediate
PTX-3	pentraxin-3
DC	dendritic cell
moDC	monocyte derived dendritic cell
Th	T helper cell
Th1	T helper cell type 1
Th2	T helper cell type 2
PBMC	peripheral blood mononuclear cell
tDC	tolerogenic dendritic cell
atDC	activated tolerogenic dendritic cell
iDC	immature dendritic cell
mDC	mature dendritic cell
LPS	lipopolysaccharides
RT	reverse transcription
PCR	polymerase chain reaction
rRNA	ribosomal ribonucleic acid
snRNA	small nuclear ribonucleic acid

Abbreviation	Meaning
TLR	Toll-like receptor
IL	interleukin
PGN	peptidoglycan
CCL	chemokine ligand
BIC gene	B cell integration cluster gene
pDC	plasmacytoid dendritic cell
MHC	major histocompatibility complex
DC-SIGN	dendritic cell-specific intercellular adhesion molecule-3-grabbing non-integrin
IFN	interferon
TNF	tumor necrosis factor

Table 17

6.2. List of Figures

6.3. Reference List

Aimanianda, V., J. Bayry, et al. (2009). "Surface hydrophobin prevents immune recognition of airborne fungal spores." Nature 460(7259): 1117-1121.

Ambion. (2011). "mirVana™ miRNA Isolation Kit." from http://www.ambion.com/techlib/prot/fm_1560.pdf.

Arasu, P., B. Wightman, et al. (1991). "Temporal regulation of lin-14 by the antagonistic action of two other heterochronic genes, lin-4 and lin-28." Genes Dev. 5(10): 1825-1833.

Bartel, D. P. (2004). "MicroRNAs: genomics, biogenesis, mechanism, and function." Cell 116(2): 281-297.

Bartel, D. P. (2009). "MicroRNAs: target recognition and regulatory functions." Cell 136(2): 215-233.

Bellocchio, S., C. Montagnoli, et al. (2004). "The contribution of the Toll-like/IL-1 receptor superfamily to innate and adaptive immunity to fungal pathogens in vivo." Journal of immunology (Baltimore, Md. : 1950) 172(5): 3059-3069.

Ben-Ami, R., R. E. Lewis, et al. (2010). "Enemy of the (immunosuppressed) state: an update on the pathogenesis of Aspergillus fumigatus infection." Br. J. Haematol. 150(4): 406-417.

Bodey, G., B. Bueltmann, et al. (1992). "Fungal infections in cancer patients: an international autopsy survey." European journal of clinical microbiology & infectious diseases : official publication of the European Society of Clinical Microbiology 11(2): 99-109.

Boeri, M., C. Verri, et al. (2011). "MicroRNA signatures in tissues and plasma predict development and prognosis of computed tomography detected lung cancer." Proc. Natl. Acad. Sci. U. S. A. 108(9): 3713-3718.

Boldin, M. P., K. D. Taganov, et al. (2011). "miR-146a is a significant brake on autoimmunity, myeloproliferation, and cancer in mice." J. Exp. Med. 208(6): 1189-1201.

Bonnett, C. R., E. J. Cornish, et al. (2006). "Early neutrophil recruitment and aggregation in the murine lung inhibit germination of Aspergillus fumigatus Conidia." Infect. Immun. 74(12): 6528-6539.

Brown, G. D. and S. Gordon (2001). "Immune recognition. A new receptor for beta-glucans." Nature 413(6851): 36-37.

Cai, X., C. H. Hagedorn, et al. (2004). "Human microRNAs are processed from capped, polyadenylated transcripts that can also function as mRNAs." RNA (New York, N.Y.) 10(12): 1957-1966.

Cenci, E., S. Perito, et al. (1997). "Th1 and Th2 cytokines in mice with invasive aspergillosis." Infect. Immun. 65(2): 564-570.

Ceppi, M., P. M. Pereira, et al. (2009). "MicroRNA-155 modulates the interleukin-1 signaling pathway in activated human monocyte-derived dendritic cells." Proc. Natl. Acad. Sci. U. S. A. 106(8): 2735-2740.

Chen, S. C.-A. and D. P. Kontoyiannis (2010). "New molecular and surrogate biomarker-based tests in the diagnosis of bacterial and fungal infection in febrile neutropenic patients." Current opinion in infectious diseases 23(6): 567-577.

Chen, T., Z. Li, et al. (2011a). "MicroRNA-146a regulates the maturation process and pro-inflammatory cytokine secretion by targeting CD40L in oxLDL-stimulated dendritic cells." FEBS Lett. 585(3): 567-573.

Chen, T., H. Yan, et al. (2011b). "MicroRNA-155 regulates lipid uptake, adhesion/chemokine marker secretion and SCG2 expression in oxLDL-stimulated dendritic cells/macrophages." Int. J. Cardiol. 147(3): 446-447.

Cortez, M. A., C. Bueso-Ramos, et al. (2011). "MicroRNAs in body fluids-the mix of hormones and biomarkers." Nature reviews. Clinical oncology.

Cortez, M. A. and G. A. Calin (2009). "MicroRNA identification in plasma and serum: a new tool to diagnose and monitor diseases." Expert opinion on biological therapy 9(6): 703-711.

Cortez, M. A., C. Ivan, et al. (2010). "microRNAs in cancer: from bench to bedside." Adv. Cancer Res. 108: 113-157.

Dai, R. and S. A. Ahmed (2011). "MicroRNA, a new paradigm for understanding immunoregulation, inflammation, and autoimmune diseases." Translational research : the journal of laboratory and clinical medicine 157(4): 163-179.

Denli, A. M., B. B. J. Tops, et al. (2004). "Processing of primary microRNAs by the Microprocessor complex." Nature 432(7014): 231-235.

Dunand-Sauthier, I., M.-L. Santiago-Raber, et al. (2011). "Silencing of c-Fos expression by microRNA-155 is critical for dendritic cell maturation and function." Blood.

Farazi, T. A., J. I. Spitzer, et al. (2011). "miRNAs in human cancer." The Journal of pathology 223(2): 102-115.

Freifeld, A. G., E. J. Bow, et al. (2011). "Clinical practice guideline for the use of antimicrobial agents in neutropenic patients with cancer: 2010 Update by the Infectious Diseases Society of America." Clinical infectious diseases : an official publication of the Infectious Diseases Society of America 52(4): 427-431.

Git, A., H. Dvinge, et al. (2010). "Systematic comparison of microarray profiling, real-time PCR, and next-generation sequencing technologies for measuring differential microRNA expression." RNA 16(5): 991-1006.

Gregory, R. I., K.-P. Yan, et al. (2004). "The Microprocessor complex mediates the genesis of microRNAs." Nature 432(7014): 235-240.

Gresnigt, M. S., M. G. Netea, et al. (2012). "Pattern recognition receptors and their role in invasive aspergillosis." Ann. N. Y. Acad. Sci. 1273: 60-67.

Hashimi, S. T., J. A. Fulcher, et al. (2009). "MicroRNA profiling identifies miR-34a and miR-21 and their target genes JAG1 and WNT1 in the coordinate regulation of dendritic cell differentiation." Blood 114(2): 404-414.

Hebart, H., C. Bollinger, et al. (2002). "Analysis of T-cell responses to Aspergillus fumigatus antigens in healthy individuals and patients with hematologic malignancies." Blood 100(13): 4521-4528.

Hohl, T. M., H. L. Van Epps, et al. (2005). "Aspergillus fumigatus triggers inflammatory responses by stage-specific beta-glucan display." PLoS pathogens 1(3): e30.

Hua, Y. J., K. Tu, et al. (2008). "Comparison of normalization methods with microRNA microarray." Genomics 92(2): 122-128.

Huntzinger, E. and E. Izaurralde (2011). "Gene silencing by microRNAs: contributions of translational repression and mRNA decay." Nature reviews. Genetics 12(2): 99-110.

InvivoGen. (2011a). "Zymosan." from http://www.invivogen.com/PDF/Zymosan_TDS.pdf.

InvivoGen. (2011b). "Zymosan Depleted." from http://www.invivogen.com/PDF/Depleted_zymosan_TDS.pdf.

Jansen, B. J., I. E. Sama, et al. (2011). "MicroRNA genes preferentially expressed in dendritic cells contain sites for conserved transcription factor binding motifs in their promoters." BMC Genomics 12: 330.

Janssen, H. L., H. W. Reesink, et al. (2013). "Treatment of HCV infection by targeting microRNA." N. Engl. J. Med. 368(18): 1685-1694.

Kota, J., R. R. Chivukula, et al. (2009). "Therapeutic microRNA delivery suppresses tumorigenesis in a murine liver cancer model." Cell 137(6): 1005-1017.

Lagos-Quintana, M., R. Rauhut, et al. (2001). "Identification of novel genes coding for small expressed RNAs." Science (New York, N.Y.) 294(5543): 853-858.

Lanzavecchia, A. and F. Sallusto (2001). "Regulation of T cell immunity by dendritic cells." Cell 106(3): 263-266.

Latgé, J. P. (1999). "Aspergillus fumigatus and aspergillosis." Clin. Microbiol. Rev. 12(2): 310-350.

Latham, G. J. (2010). "Normalization of microRNA quantitative RT-PCR data in reduced scale experimental designs." Methods in molecular biology (Clifton, N.J.) 667: 19-31.

Lee, R. C., R. L. Feinbaum, et al. (1993). "The C. elegans heterochronic gene lin-4 encodes small RNAs with antisense complementarity to lin-14." Cell 75(5): 843-854.

Lee, Y., C. Ahn, et al. (2003). "The nuclear RNase III Drosha initiates microRNA processing." Nature 425(6956): 415-419.

Lee, Y., M. Kim, et al. (2004). "MicroRNA genes are transcribed by RNA polymerase II." The EMBO journal 23(20): 4051-4060.

Levitz, S. M. (2004). "Interactions of Toll-like receptors with fungi." Microbes and infection / Institut Pasteur 6(15): 1351-1355.

Levitz, S. M. and T. P. Farrell (1990). "Human neutrophil degranulation stimulated by Aspergillus fumigatus." J. Leukoc. Biol. 47(2): 170-175.

Li, L., X.-P. Chen, et al. (2010). "MicroRNA-146a and human disease." Scand. J. Immunol. 71(4): 227-231.

Lindsay, M. A. (2008). "microRNAs and the immune response." Trends in immunology 29(7): 343-351.

Liu, X., Z. Zhan, et al. (2010). "MicroRNA-148/152 impair innate response and antigen presentation of TLR-triggered dendritic cells by targeting CaMKIIalpha." J. Immunol. 185(12): 7244-7251.

Livak, K. J. and T. D. Schmittgen (2001). "Analysis of relative gene expression data using real-time quantitative PCR and the 2(-Delta Delta C(T)) Method." Methods (San Diego, Calif.) 25(4): 402-408.

Lu, C., X. Huang, et al. (2011). "MiR-221 and miR-155 regulate human dendritic cell development, apoptosis and IL-12 production through targeting of p27kip1, KPC1 and SOCS-1." Blood.

Lu, L. F., T. H. Thai, et al. (2009). "Foxp3-dependent microRNA155 confers competitive fitness to regulatory T cells by targeting SOCS1 protein." Immunity 30(1): 80-91.

Mambula, S. S., K. Sau, et al. (2002). "Toll-like receptor (TLR) signaling in response to Aspergillus fumigatus." The Journal of biological chemistry 277(42): 39320-39326.

Marr, K. A. (2010). "Fungal infections in oncology patients: update on epidemiology, prevention, and treatment: REVIEW." Curr. Opin. Oncol. 22(2): 138-142.

Martinez-Nunez, R. T., F. Louafi, et al. (2009). "MicroRNA-155 modulates the pathogen binding ability of dendritic cells (DCs) by down-regulation of DC-specific intercellular adhesion molecule-3 grabbing non-integrin (DC-SIGN)." The Journal of biological chemistry 284(24): 16334-16342.

Meier, A., C. J. Kirschning, et al. (2003). "Toll-like receptor (TLR) 2 and TLR4 are essential for Aspergillus-induced activation of murine macrophages." Cellular microbiology 5(8): 561-570.

Mestdagh, P., P. van Vlierberghe, et al. (2009). "A novel and universal method for microRNA RT-qPCR data normalization." Genome biology 10(6): R64.

Meyer, S. U., M. W. Pfaffl, et al. (2010). "Normalization strategies for microRNA profiling experiments: a 'normal' way to a hidden layer of complexity?" Biotechnology letters 32(12): 1777-1788.

Nahid, M. A., M. Satoh, et al. (2011). "Mechanistic role of microRNA-146a in endotoxin-induced differential cross-regulation of TLR signaling." Journal of immunology (Baltimore, Md. : 1950) 186(3): 1723-1734.

Nahid, M. A., B. Yao, et al. (2013). "Regulation of TLR2-mediated tolerance and cross-tolerance through IRAK4 modulation by miR-132 and miR-212." J. Immunol. 190(3): 1250-1263.

Netea, M. G., J. W. M. van der Meer, et al. (2006). "Role of the dual interaction of fungal pathogens with pattern recognition receptors in the activation and modulation of host defence." Clinical microbiology and infection : the official publication of the European Society of Clinical Microbiology and Infectious Diseases 12(5): 404-409.

Netea, M. G., A. Warris, et al. (2003). "Aspergillus fumigatus evades immune recognition during germination through loss of toll-like receptor-4-mediated signal transduction." J. Infect. Dis. 188(2): 320-326.

O'Connell, R. M., A. A. Chaudhuri, et al. (2009). "Inositol phosphatase SHIP1 is a primary target of miR-155." Proc. Natl. Acad. Sci. U. S. A. 106(17): 7113-7118.

O'Connell, R. M., D. Kahn, et al. (2010a). "MicroRNA-155 promotes autoimmune inflammation by enhancing inflammatory T cell development." Immunity 33(4): 607-619.

O'Connell, R. M., D. S. Rao, et al. (2010b). "Physiological and pathological roles for microRNAs in the immune system." Nature reviews. Immunology 10(2): 111-122.

O'Connell, R. M., K. D. Taganov, et al. (2007). "MicroRNA-155 is induced during the macrophage inflammatory response." Proc. Natl. Acad. Sci. U. S. A. 104(5): 1604-1609.

O'Neill, L. A., F. J. Sheedy, et al. (2011). "MicroRNAs: the fine-tuners of Toll-like receptor signalling." Nature reviews. Immunology 11(3): 163-175.

Pedersen, I. M., D. Otero, et al. (2009). "Onco-miR-155 targets SHIP1 to promote TNFalpha-dependent growth of B cell lymphomas." EMBO Mol Med 1(5): 288-295.

Peltier, H. J. and G. J. Latham (2008). "Normalization of microRNA expression levels in quantitative RT-PCR assays: identification of suitable reference RNA targets in normal and cancerous human solid tissues." RNA (New York, N.Y.) 14(5): 844-852.

Perry, M. M., S. A. Moschos, et al. (2008). "Rapid changes in microRNA-146a expression negatively regulate the IL-1beta-induced inflammatory response in human lung alveolar epithelial cells." J. Immunol. 180(8): 5689-5698.

Person, A. K., D. P. Kontoyiannis, et al. (2010). "Fungal infections in transplant and oncology patients: SCIENCEDIRECT 30$." Infect. Dis. Clin. North Am. 24(2): 439-459.

Philippe, B., O. Ibrahim-Granet, et al. (2003). "Killing of Aspergillus fumigatus by alveolar macrophages is mediated by reactive oxidant intermediates." Infect. Immun. 71(6): 3034-3042.

Pradervand, S., J. Weber, et al. (2009). "Impact of normalization on miRNA microarray expression profiling." RNA 15(3): 493-501.

Rex, J. H., J. E. Bennett, et al. (1990). "Normal and deficient neutrophils can cooperate to damage Aspergillus fumigatus hyphae." The Journal of infectious diseases 162(2): 523-528.

Rodriguez, A., E. Vigorito, et al. (2007). "Requirement of bic/microRNA-155 for normal immune function." Science 316(5824): 608-611.

Sato, F., S. Tsuchiya, et al. (2009). "Intra-platform repeatability and inter-platform comparability of microRNA microarray technology." PloS one 4(5): e5540.

Segal, B. H. (2009). "Aspergillosis." The New England journal of medicine 360(18): 1870-1884.

Serrano-Gómez, D., A. Domínguez-Soto, et al. (2004). "Dendritic cell-specific intercellular adhesion molecule 3-grabbing nonintegrin mediates binding and internalization of Aspergillus fumigatus conidia by dendritic cells and macrophages." Journal of immunology (Baltimore, Md. : 1950) 173(9): 5635-5643.

Shaked, I., A. Meerson, et al. (2009). "MicroRNA-132 potentiates cholinergic anti-inflammatory signaling by targeting acetylcholinesterase." Immunity 31(6): 965-973.

Sun, Y., S. Varambally, et al. (2011). "Targeting of microRNA-142-3p in dendritic cells regulates endotoxin-induced mortality." Blood 117(23): 6172-6183.

Taganov, K. D., M. P. Boldin, et al. (2007). "MicroRNAs and immunity: tiny players in a big field." Immunity 26(2): 133-137.

Taganov, K. D., M. P. Boldin, et al. (2006). "NF-kappaB-dependent induction of microRNA miR-146, an inhibitor targeted to signaling proteins of innate immune responses." Proc. Natl. Acad. Sci. U. S. A. 103(33): 12481-12486.

Thai, T. H., D. P. Calado, et al. (2007). "Regulation of the germinal center response by microRNA-155." Science 316(5824): 604-608.

Tserel, L., T. Runnel, et al. (2011). "MicroRNA expression profiles of human blood monocyte-derived dendritic cells and macrophages reveal miR-511 as putative positive regulator of Toll-like receptor 4." J. Biol. Chem. 286(30): 26487-26495.

Tsitsiou, E. and M. A. Lindsay (2009). "microRNAs and the immune response." Curr Opin Pharmacol 9(4): 514-520.

van Rooij, E. (2011). "The art of microRNA research." Circ. Res. 108(2): 219-234.

Vigorito, E., K. L. Perks, et al. (2007). "microRNA-155 regulates the generation of immunoglobulin class-switched plasma cells." Immunity 27(6): 847-859.

Walsh, T. J., E. J. Anaissie, et al. (2008). "Treatment of aspergillosis: clinical practice guidelines of the Infectious Diseases Society of America." Clinical infectious diseases : an official publication of the Infectious Diseases Society of America 46(3): 327-360.

Wang, J. E., A. Warris, et al. (2001). "Involvement of CD14 and toll-like receptors in activation of human monocytes by Aspergillus fumigatus hyphae." Infect. Immun. 69(4): 2402-2406.

Wang, P., J. Hou, et al. (2010). "Inducible microRNA-155 feedback promotes type I IFN signaling in antiviral innate immunity by targeting suppressor of cytokine signaling 1." J. Immunol. 185(10): 6226-6233.

Wightman, B., T. R. Bürglin, et al. (1991). "Negative regulatory sequences in the lin-14 3'-untranslated region are necessary to generate a temporal switch during Caenorhabditis elegans development." Genes Dev. 5(10): 1813-1824.

Wightman, B., I. Ha, et al. (1993). "Posttranscriptional regulation of the heterochronic gene lin-14 by lin-4 mediates temporal pattern formation in C. elegans." Cell 75(5): 855-862.

Williams, A. E., M. M. Perry, et al. (2008). "Role of miRNA-146a in the regulation of the innate immune response and cancer." Biochem. Soc. Trans. 36(Pt 6): 1211-1215.

Xiao, C. and K. Rajewsky (2009). "MicroRNA control in the immune system: basic principles." Cell 136(1): 26-36.

Yi, R., B. P. Doehle, et al. (2005). "Overexpression of exportin 5 enhances RNA interference mediated by short hairpin RNAs and microRNAs." RNA (New York, N.Y.) 11(2): 220-226.

Yi, R., Y. Qin, et al. (2003). "Exportin-5 mediates the nuclear export of pre-microRNAs and short hairpin RNAs." Genes Dev. 17(24): 3011-3016.

Zarember, K. A., J. A. Sugui, et al. (2007). "Human polymorphonuclear leukocytes inhibit Aspergillus fumigatus conidial growth by lactoferrin-mediated iron depletion." Journal of immunology (Baltimore, Md. : 1950) 178(10): 6367-6373.

Zhang, M., F. Liu, et al. (2011). "Inhibition of microRNA let-7i depresses maturation and functional state of dendritic cells in response to lipopolysaccharide stimulation via targeting suppressor of cytokine signaling 1." J. Immunol. 187(4): 1674-1683.

Zhao, J. L., D. S. Rao, et al. (2011). "NF-kappaB dysregulation in microRNA-146a-deficient mice drives the development of myeloid malignancies." Proc. Natl. Acad. Sci. U. S. A. 108(22): 9184-9189.

Zhou, H., X. Huang, et al. (2010). "miR-155 and its star-form partner miR-155* cooperatively regulate type I interferon production by human plasmacytoid dendritic cells." Blood 116(26): 5885-5894.

Danksagung

Mein besonderer Dank gilt folgenden Personen:

- Priv.-Doz. Dr. Jürgen Löffler für die Vergabe des interessanten Themas und die herausragende Betreuung und Unterstützung während der ganzen Zeit.
- Prof. Dr. Hermann Einsele für die Ermöglichung und Unterstützung der Arbeit.
- Helga Sennefelder für die Einarbeitung in die Labormethoden.
- Allen Mitarbeitern der AG Löffler für die gute Zusammenarbeit.